Universiteit Twente, in collaboration with Elisabeth-Tweesteden Ziekenhuis (ETZ)

Distal radius fracture management

Using 3D printed, in-house design, production, and implementation of wrist cast/orthosis for the treatment of distal radius fractures.

Koen Storck

2021-2022

Distal radius fracture management

Using 3D printed, in-house design, production, and implementation of wrist cast/orthosis for the treatment of distal radius fractures.

Author	K.C.G. Storck, Bsc. (Koen) Technical Medicine – Medical Imaging and Intervention
Graduation committee	
Chairman	Prof.dr.ir. C.H. Slump Faculty of Electrical Engineering, Mathematics and Computer Science (EEMCS) | University of Twente | Enschede
Medical supervisor:	Drs. M. Bemelman Trauma surgery| ETZ hospital | Tilburg
	Dr. L. Brouwers Trauma surgery| ETZ hospital | Tilburg
Technical supervisor UT:	Prof.dr.ir. C.H. Slump Faculty of Electrical Engineering, Mathematics and Computer Science (EEMCS) | University of Twente | Enschede
Process Supervisor UT:	Drs. R.M. Krol Faculty of Science and Technology (ET) | University of Twente | Enschede
	Drs. B.J.C.C. Hessink- Sweep Faculty of Science and Technology (ET) | University of Twente | Enschede
External member:	L. van de Velde, Msc (Lennart) Multi-Modality Medical Imaging (M3I) | University of Twente | Enschede

Colloquium

Date:	December 20th 2022
Time:	12:30 PM
Place:	RA3237 in de Ravelijn te Enschede

Acknowledgments

My student career is coming to an end after a little over ten years. During this period, I have learned a lot for what I am grateful for. Fifteen months ago, I started my Technical Medicine Master's adventure in Tilburg. This year was challenging, I could not have done it without the support of several people

First, I would like to thank the Anatomy department at the University Hospital in Utrecht (UMCU) for their cooperation during the cadaver study and for making the cadaver pieces available for this research. Secondly, I'd like to thank the Radiology department, the employees of the plaster room, and the morgue in the Elisabeth-Two Cities hospital for their help during this research. I also want to thank the staff of the surgical department. Your uplifting conversations helped me to stay motivated.

A big thanks also goes to my colleagues in the ETZ 3D lab. Annabel, Pieter-Jan, and Vito. You guys provided a cozy environment, positive energy, laughter, and the necessary coffee breaks. A special thanks to my friends, especially Yordi. You helped me a lot with tips and tricks, and the brainstorming sessions.

Moreover, a huge thanks goes to my peer-to-peer coaching group. As a pre-master student, you don't get the chance to build a relationship as you shift between subjects from different years. Therefore, I did not know any of you guys. However, from the first moment, it felt secure and safe with all of you. I have learned a lot during our meetings. Thank you for the chance to learn, and thanks for helping to get to know me.

Thanks to Bregje and Ruby (process supervisors). During the M2-internship, Bregje helped me to stay motivated and helped me in my personal development. Ruby, a big thanks to you. Normally I am not open to someone I do not know. Now, after one year, you have given me a lot of skills to be more open and to be more in touch with myself. You provide an open and safe environment for people to say what they want and not be judged.

I want to thank my family for the support and for trying to understand what I do, and for listing to me when I complained. This year was hard and I certainly could not have dealt with it if was not for the support of my girlfriend. I was not always happy when I came home, but you almost always turned my frown to a smile. Thanks for listening to my complaints, for the cuddle when I needed it, but most of all for endlessly having my back. I love you.

Lastly, I would like to thank the supervisors (Mike Bemelman, Lars Brouwers, and Kees Slump). Your advice, coaching, and feedback helped me to become a better technical physician. You helped me to look at my reports from a different angle. You gave me a chance to learn new skills, which I used for my thesis. My thesis would not be so complete without your efforts and feedback. The thesis was not easy to complete. When I saw drawbacks, you saw opportunities, which helped me forward. I learned a lot from your mindset, which will certainly help me in my future career.

It was an intense year, but as I have learned: "Hakuna matata" – L.Brouwers.
For the future I will try to live a bit more by the saying 'Take it easy as easy does it`.

I hope you enjoy reding my thesis.
Wishing you all the best,

Koen Storck

Summary

INTRODUCTION

Distal radius fractures (DRF) are traditionally treated with plaster casts, which have disadvantages. Up to 30% of plaster casting leads to complications. The 3D-printed cast could overcome these issues: they are lightweight, waterproof, open-latticed. Literature showed no consensus about the materials, printers, design, and implementation in the clinic for 3D-printed casts. The aim was to investigate the feasibility of 3D printed casts, the implementation of 3D casts for the treatment of distal radius fractures, and to characterize the magnitude of fracture displacement during static load in human cadaver models with Colles fractures.

METHODS

Multiple sub-studies were performed. Material tests were conducted to select the most suitable design and material. A workflow was designed to test feasibility and implementation in the clinic. A pilot study was conducted to assess three aspects of 3D casts treatment: the feasibility of the implementation of 3D-printed casts, the clinical outcomes, and patient experiences. A final step was the human model cadaver study, where a static load was placed on the casts to see if the cast could prevent secondary displacement of the DRF in a cadaver model.

RESULTS

The material tests showed PLA was the best material to print with Fused deposition modeling (FDM).ith a semi-automated design, printable casts were created. The casts could be printed within 24-48 hours. The pilot study showed it is feasible to treat a patient within 24 hours after admission to the ER. Three children with greenstick or buckle/torus fractures were successfully treated with 3D-printed casts. The treatment scored 9.0 out of 10.0. The human cadaver model study showed displacement in the models if a static load is placed on them.

CONCLUSION

A lightweight, water-resistant, and ventilated cast can be designed and printed within 24-48 hours. The wrist casts ensure adequate immobilization, comfort and can be implemented for greenstick and buckle/torus fractures. The human cadaver model study showed displacement after applying static loads. However, this study ignores the compensation mechanism (muscle contraction and relaxation) of the lower arm. Therefore, more research is necessary. Also, research is needed to estimate swelling more accurately to make the cast fit perfectly. In the future, 3D-printed casts for other fractures (stable and unstable fractures in the lower and upper extremities), and 3D-printed orthosis/braces in the field of orthotics should also be explored.

List of abbreviations

Activity of daily living	ADL
Carpometacarpal joint	CMC
Digital light processing	DLP
Distal radioulnar joint	DRUJ
Distal radius fracture	DRF
Electronic patient dossier	EPD
Elisabeth Tweesteden Hospital	ETZ
Emergency room	ER
Fused deposition modeling	FDM
Medical ethics review committee	METC
Metacarpophalangeal joint	MCP
Non-uniform rational basis spline	NURBS
Philips Intellispace Portal	PIP
Radiocarpal joint	RCJ
Randomized controlled trial	RCT
Range of motion	ROM
Selective Laser Sintering	SLS
Standard Triangle Language	STL
Ulnocarpal joint	UCJ
Ultraviolet	UV
Visual Analogue Scale	VAS
Quality of Life	QoL

Content

Introduction

Anatomical Background

The arm consists of the upper arm, the lower arm, and the hand. The radius, ulna, and carpal bones are part of the wrist joint, a complex anatomical structure. In total, the wrist is made up of fifteen bones and various supporting structures (complex composition of muscles, tendons and ligaments, a nerve system, and vascularization). The wrist joint is a combination of three joints: the radiocarpal joint (RCJ), ulnocarpal joint (UCJ), and distal radioulnar joint (DRUJ) [1], [2]. These three joints form an ellipsoid joint that generates six motions ((palmar) flexion, (dorsal) extension, radial deviation, ulnar deviation, and pro and supination). Each movement has a particular range of motion (ROM) (described in Table 1). The radius and ulna form a rolling joint that can move the hand in pronation and supination [3]. The bony anatomy of the wrist bones is shown in Figure 1.

Table 1: Range of motion of wrist movements [2], [3].

Movement	Range of Motion (in Degree)
Flexion	80-90°
Extension	60-70°
Radial deviation	15-20°
Ulnar deviation	30-40°
Pronation	70-90°
Supination	85-95°

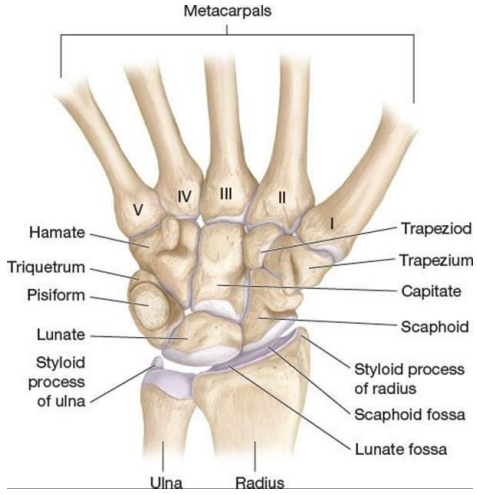

Figure 1: Bony anatomy of the wrist bones [4].

Fractures

"A fracture is a breach in the structural continuity of the bone cortex, with a degree of injury to the surrounding soft tissues." [5] Or simplified, a bone fracture is a complete or incomplete discontinuity of bone [6]. Fractures are expressed in many different ways, therefore fractures are classified. Classification is essential for communication, treatment decisions, prognosis and to compare results [7], [8].

One of the most used fracture classification systems is the AO/OTA Classification of Fractures and Dislocations [6]. This system defines fractures in; which bone is fractured, where the fracture is located (proximal, diaphysis, or distal), and whether the fracture is extra-articular (the fracture line can be metaphyseal or epiphyseal, but there is no extension into the articular surface), or intra-articular (has an extension into the articular surface) [9].

Further, there are universal modifiers. These are descriptive terms of fracture morphology, displacement, associated injury, and location that are applicable to most fractures [10]. This is a lengthy list of terms of which the most important terms are: (non)displaced and dislocated. A displaced fracture is when the ends of the bone of the fracture site are not aligned (displaced is also an unstable fracture). However, 'displaced' is a broad and comprehensive term. A more descriptive and scientific description of a dislocated or unstable fracture is:

- Dorsal tilt > 15° on lateral radiograph (Colles fracture) [11]
- Volar tilt > 20° on lateral radiograph (Smith's or reversed Barton's fracture) [11], [12]
- Shortening of distal end of the radius > 5 mm in relation to the distal end of the ulna in posterior-anterior (PA) direction [11]
- Intra-articular step off > 2 mm [11]
- Radial inclination < 15° in AP on radiograph [11]
- Subluxation of the lunate [11]

Distal radius fractures

In this study, the distal radius fracture (DRF) is the main object of interest. DRFs are one of the most common types of fractures accounting for up to 25% of all the fractures [13], [14]. The incidence of DRFs in the Netherlands is 20 to 40 per 10,000 persons each year [15]. The distal radius can be fractured in many ways. The more common fractures have been given a name (see Figure 2 for visual support):

- Colles fracture; which is an extra-articular fracture of the distal metaphysis of the radius with dorsal angulation. Normally this is an uncomplicated and stable fracture. It is one of the most frequent DRF [13]. This fracture is mostly caused by a fall forward with an outstretched hand. [6]
- Smith's fracture; is an extra-articular fracture and is the result of high-energy trauma on the volar flexed wrist. This is, in most cases, an unstable fracture where surgery is needed to stabilize the fracture. [6]
- Die-punch fracture; is a depression fracture of the lunate fossa of the distal radius. This fracture occurs as a result of a transverse load through the lunate. [6]
- Barton's fracture; is expressed in two ways. The volar-type Barton is a fracture-dislocation of the volar rim of the radius. This occurs more often than the dorsal-type Barton, which is a fracture-dislocation of the dorsal rim of the radius. Both fractures are intra-articular. The hallmark of this fracture is the dislocation of the radiocarpal joint. Surgery is always necessary unless the fractured bone is too small to attach to the radius. [6]
- Chauffeur's fracture; is a fracture caused by too much pressure of the scaphoid on the radial styloid process that causes avulsion of the radial styloid. If the fracture is displaced, then reduction is needed. [6]

Treatment

The first step taken when a patient comes into the emergency room (ER) is a physical examination (swelling, sometimes visible angular deviation, (pressure) pain) [16]. Based on the observation, a radiographic image/CT scan (anterior-posterior and lateral direction) can be made [16]. The X-ray/CT images may confirm or rule out a DRF. Depending on the fracture, a treatment plan is executed. If the DRF is displaced, then the reduction is needed, which can be performed open or closed. The preferred option is closed reduction, in this case, there is no surgery. If this is not possible, then open reduction is considered. Reduction of the unstable/displaced fracture is performed and, if needed, bone fragments and debris can be removed. When open reduction is executed, often a fixed metal (volar) plate is used to stabilize the bones in their anatomical position [17]. A closed reduction is performed with external forces on the fracture to realign the fracture ends. A plaster cast is used to relieve pain and to hold the

anatomical position of the bones for 3-5 weeks. In case of stable non-displaced fracture, plaster for one week is sufficient for pain relief [18], [19]. Plaster casting after open reduction is generally not done.

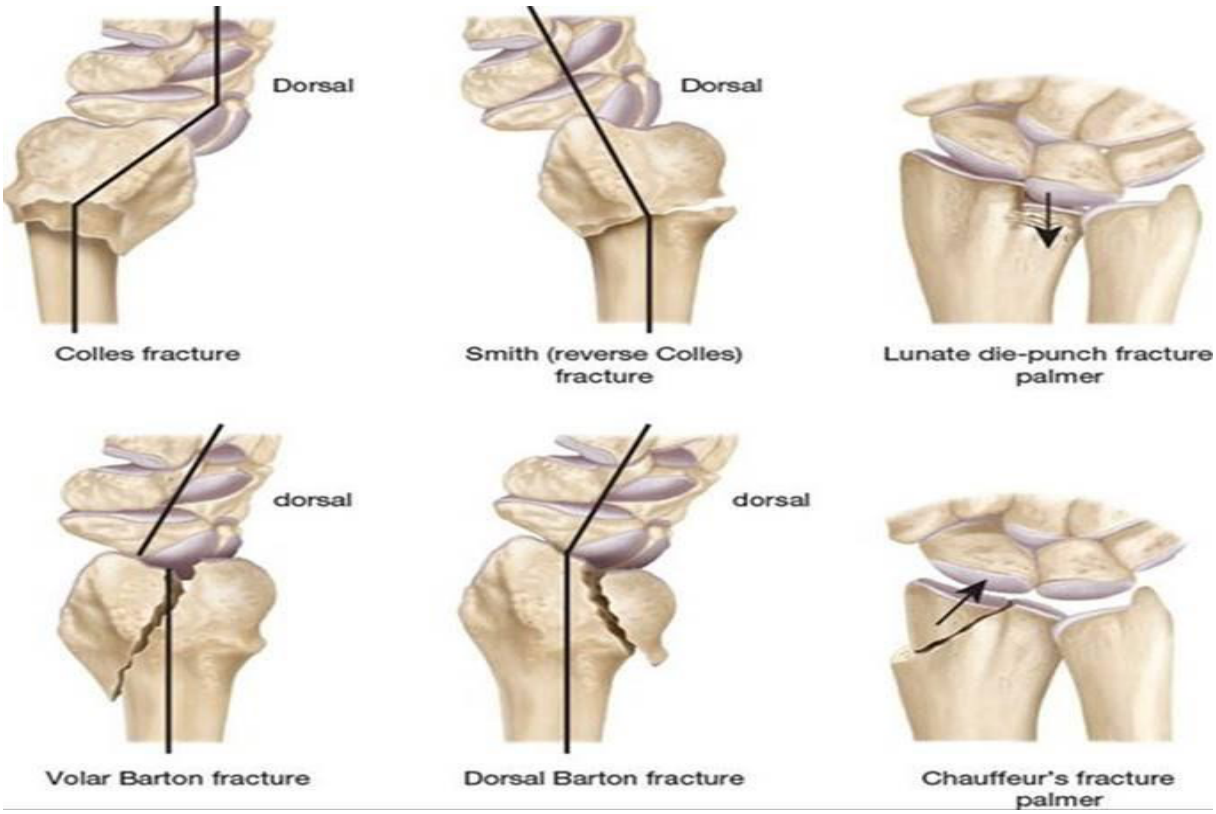

Figure 2, the image of frequent fracture types of DRF [4].

Problem

DRFs are generally immobilized with a plaster cast for 3-5 weeks (3 weeks for stable fractures and 4-5 weeks for unstable fractures) [20]. Plaster casting is cheap and a reliable way for immobilization of the fracture, however, it has its disadvantages.

- The first disadvantage is that plaster casts are not waterproof. Thus showering, bathing, or ultimately swimming without special measures is not possible [21].
- Plaster casts can give pressure sores and plaster is associated with compartment syndrome [22], [23]. In all cases with cast immobilization up to 30% experience complications or problems [23]–[25].
- The lack of the possibility of cleaning and ventilation of the arm in the plaster complicates hygiene, it may increase sweating and can result in skin problems and itching [21], [22], [24], [26], [27]
- Another disadvantage of a cast is that it restricts the visual inspection of the skin. This increases the risk of not detecting or late detection of, mainly skin-related, complications [19], [21].
- A disadvantage often overseen, is the weight of the plaster casts (A plaster casts weights approximately 500 gram [28]). It can cause pain (in the neck or back), result in muscle loss, decreases muscle strength [29], and possible temporary inactivity resulting in a decreased optimal healing process and stiffness. Muscle loss always occurs during the healing process of

a fracture, the average loss of strength after 3-4 weeks is 13.3% [30]. The need for fixation means that certain muscle groups are inevitably restricted in their movement.

There are alternatives to plaster casts like splinting or bandage. These may be used in the case of an intrinsic stable fracture.[26], [31]–[36] However, these alternatives bring along the same hygiene and inspectional issues as traditional plaster casting [21], [37], although it has some advantages over plaster casts mainly in terms of weight and comfort which leads to improved patient satisfaction [26], [32].

Another alternative to plaster cast treatment is to use CAD/CAM technology to manufacture customized 3D-printed orthoses. This can be done with lighter materials. [28]. A lighter cast could solve the weight problems associated with plaster cast, such as pain, stiffness, and discomfort [19], [21], [26], [28], [38]. Furthermore, the weight of the plastic cast can prevent muscle loss due to muscle inactivity caused by the weight of the plaster cast. Therefore, in total plastic cast could prevent or decrease pain, muscle loss, and discomfort.

Introduction 3D printing

The application of 3D printing in medicine is currently becoming increasingly popular. Here in the Elisabeth-Tweesteden Hospital (ETZ) 3D printing is used for preoperative management/clinical workflow (more specifically, trauma and maxillofacial surgery, etc.). 3D-printed (anatomical) models are used for surgical planning, training or education, and personalized treatment [39]. The use of these models leads to a more precise treatment and a better understanding of the medical problem [28], [39], [40]. 3D printing allows three-dimensional renderings to be realized as physical objects with the use of a 3D printer, thus directing the medicine in a more personalized approach. There are different techniques in 3D printing, available at the ETZ:

- The Formlabs (Formlabs Inc., Somerville, MA, USA) is a 3D printer that uses the stereolithography (SLA) technique. With SLA, a liquid resin gets cured/hardened in a vat by ultraviolet (UV) light. This process is called *Vat Polymerization* and cures each microfine resin layer using UV light precisely directed by mirrors. The materials used for SLA printing are thermoset polymers. This is a viscous liquid prepolymer (resin) that is irreversibly hardened/cured by heat.
- The Ultimaker (Ultimaker B.V., the Netherlands) is a printer that uses a technique called Fused Deposition Modelling (FDM), which is a form of material extrusion. Spooled polymers are extruded or compressed through a heated nozzle mounted on a movable arm. The nozzle moves horizontally while the bed moves vertically, allowing the melted material to be built layer after layer. Proper adhesion between layers occurs through precise temperature control or the use of chemical bonding agents. The advantage of FDM is that it offers a relatively cheap manner to produce medical models and many materials can be used (mainly thermoplastics and composites).

In this thesis, we want to explore the possibilities of 3D printing of casts which can solve/reduce the problems associated with plaster castings. 3D printing can be an alternative with possibilities to create an open latticed, waterproof, and lightweight cast. In the past years, multiple companies have printed 3D casts to immobilize the wrist with injuries, fractures, and arthritis [24], [28], [41]. However, these companies have not tested scientifically if these casts provide sufficient immobilization for healing, improved comfort, whether the casts are safe, and can prevent (secondary) displacements.

Study goal and research question

The aim of this thesis is to address the problems of treating DRFs with plaster casts: Not waterproof, lack of hygiene, muscle loss due to inactivity, and sores. Therefore, a design of a cast that is open, lightweight, and strong/stiff would be ideal. One way to achieve this is with 3D printing. Different companies (Xkelet, ActivArmor, Castprint) have tried to print 3D casts as an alternative to the conventional plaster cast. These casts have been used for immobilizing (DRF) fractures. However, these companies show only the results, not how these results are achieved. Further, it remains unknown which forces the casts should withstand if the fractures were immobilized enough to prevent (secondary) displacements, impairment in the activity of daily living (ADL), the consensus about which material to use, and the safety of the patients.

In this thesis, the goal will be to investigate whether 3D casts can replace plaster casts with non-displaced DRFs (extra-articular (AO 23-A2.2) while this fracture is mostly treated with plaster casts). Therefore, a literature study will be conducted to investigate which requirements the 3D cast for DRF has to be met and which material is sufficient or equal to plaster to use for the cast. Furthermore, a pilot study is conducted to gain knowledge about if the cast is safe, comfortable, and feasible for the patient and the clinic. For the pilot study, a clinical workflow must be designed and analyzed on how this will fit into the clinical practice. Additionally, a test setup will contribute to investigating whether the 3D casts are suitable for replacing plaster casts. In this test environment, a static load will be placed on the casts to see if the cast could prevent secondary displacement of the DRF (AO 23-A2.2) in a cadaver model.

Technical background

The current chapter encompasses an introduction on the production of an orthosis. The chapter starts with the research of choosing the material for an orthosis, followed by the technical procedure of scanning the arm, the designing phase and concluding with the printing process of the orthosis.

3D printing

The current study uses the fused deposition modeling (FDM) Ultimaker (S3 and/or S5) to print a cast. Casts printed with FDM have previously been compared to casts printed with SLA [42], [43]. SLA has been shown to create an inferior surface quality. However, we still opted for the FDM printer based on cost-effectiveness because the cast is used once and will be thrown away after six-twelve weeks [11], [42]–[46]. Chae *et al.* and Kim *et al.* described that FDM has a higher labor-intensive post-processing process for FDM printed products [47]–[49]. The surface finish of an FDM product is of lower quality than SLA products. However, with surface smoothing, the surface quality improves tremendously while the cost is lower compared to SLA printing. [47]–[49]. Another option, if sanding is no option, is to attach a soft material on the inside of the cast to ensure soft contact.

3D Printing settings

3D printing starts with a digital file processed into a three-dimensional solid object by additive processes. Objects are produced by building layer upon layer until the entire object is produced. Each layer can be seen as a thinly sliced horizontal cross-section of the object [50]. The quality of the 3D print depends on the printer settings, including infill, line thickness, and patron of infill. Furthermore, the orientation of the model and the kind of material influences the quality of the 3D print. An aim of the current study is to investigate the optimal printing settings to obtain a cast with the optimal strength combined with optimal printing time in relation to the desired design of the casts.

Influence of 3D print settings

The (mechanical) properties of the 3D-printed object are partly defined by the settings. The primary process parameters which influence the properties of the print are raster angle, layer orientation, layer thickness, and infill density [51]. Table 2 shows the primary settings, functions, and the influence these parameters exert on the print.

In a study from Tanveer *et al.*, it was shown that there is a positive relationship between density of the print and the peak load [51]. A higher density leads to better bonding of adjacent layers resulting in a stronger structure. However, a less dense infill shows greater flexibility, consequently resulting in the material being able to flex more before breaking.

In the printing process, the nozzle will move in the direction of the X-axis and Y-axis (or a combination of these directions), while the platform will move in the direction of the Z-axis to build the object layer by layer. Hanon *et al.* tested the properties of printed material in 3 directions (raster directions: 0°, 45°, and 90°). [52] It was shown that printing at a 45° angle provides the best strength and flexural properties when forces are applied perpendicular to the tested model. Furthermore, it was shown that printing in alternating layer directions resulted in more strength by printing in a 45° and -45° direction. [52]

Dwiyati *et al.* have studied the influence of layerthickness on the tensile strength of the material [53]. It was shown that the molecules in one layer are greater than the tensile strength interlayers. This can be explained due to the characteristics within each layer. The polymer molecules within the layer

have the same printing conditions of heating and cooling which results in a stronger bonding of the polymer molecules. The thicker the layer the stronger the bond, this is because more polymer chains are involved in forming bonds. In the study of Dwiyati *et al.* the thickness of 0.3 mm showed the greatest force and tensile strength compared to thickness 0.1 mm and 0.2 mm. [53]

These results cannot directly be translated to the application of the casts, due to its cylindrical shape. However, these results can help in the design and printing of the casts.

Table 2 Properties of the printer settings

Setting	Function	Effect on properties	Source
Density	Is the percentage of infill of the space inside perimeters (is the number of layers of the external side of the print) and solid layers (are the numbers of layers of the top and bottom part of the print)?	In Wikla *et al.*, is tested what an increasing percentage (10% -25% - 40% - 60%) influence has on its tensile strength. It is shown that 60% has the strongest properties. In Hanon *et al.*, the difference between 50% and 100% infill is shown to have a significant effect on the strength properties, for 100% almost two times stronger.	[52], [54]
Raster orientation	The printing direction of the internal parts. This can be printed in the 0°, 45°, and 90° directions.	Literature has shown that the printing direction of 45° will give the strongest properties.	[52], [53], [55]
Layers orientation	Successive layers can be printed in the same direction but also be varied. E.g. if the raster direction in the first layer is 45° the second layer could be build at -45°.	In Hanon *et al.*, it is shown that by alternating the rasters direction per layer, the properties will gain strength. The sample with 45°/-45° has the best properties, second best is the print with raster direction in 45° direction.	[52]
Layer thickness	This is the thickness of the layer extruded by the nozzle of the 3D printer.	In Dwiyati *et al.* is shown that the thicker the layer stronger the print is.	[53]

Designing process

Requirements

The design must fulfill a few requirements. The design must have similar stabilization abilities as traditional plaster or better. Therefore, the design must be rigid and not break during activities of daily living or break after a small impact. Plaster casts do not allow for visual inspection and ventilation. Furthermore, plaster complicates hygiene due to increased sweating. Up to 30% of the cases of plaster treatments, skin-related complications are present [23], [24]. A design with openings can resolve the problem with ventilation and visual inspection and could decrease the number of skin-related problems. The cast must be fenestrated to allow for visual skin inspection and increase hygiene and provide a higher comfort for the patient. Furthermore, the openings lead to less material which results in a lower weight which is also beneficial. The fenestrated design could decrease above mentioned skin-related complications: decreased hygiene, prevention or decrease the cases of pressure sores, over-compression of the limb, as well as swollen fingers, and pain due to inadequate fit. These complaints are often associated with plaster casting [22], [23]. With the utility of 3D scanning and post-processing, it is possible to allow for swelling in the first days after the trauma.

The openings have a pattern, this pattern must retain the strength of the orthosis. In literature, many options have been described: Voronoi, droplet, round holes, swirl pattern, orthogonal, honeycomb, diamond-shaped holes, and a hexagonal pattern [21], [38], [42]–[46], [56]–[61]. Several studies have shown that the Voronoi pattern is the best candidate for an orthosis, as it provides the best stiffness, which is essential to immobilize the fracture during the treatment and is crucial for the healing process [60], [61]. The optimal pattern is created by balancing the number and size of the holes

(balance between optimal stiffness and ventilation). A cast with larger holes will provide more ventilation and allow better visual inspection of the skin but will have reduced stiffness and vice versa.

Plaster casts are not water-resistant, which complicates the hygiene of the patient. However, showering is possible with special measures in place [38]. 3D printed materials are mostly made from plastics and are water-resistant. The possibility of showering provides better hygiene [38]. Another advantage of 3D printed materials is that plastics are light. A plaster cast weighs around 500 grams, and patients often complain about the weight [28]. Other important conditions include safety and costs. The material must not be cytotoxic or give skin reactions (sensitizing or irritating), according to ISO 10993-1. Furthermore, the costs and printing time is important in choosing the right material. Both should be as low as possible.

The production and design of the cast should have as few steps as possible. The workflow should be easy to follow and should take the lowest time possible. This will improve the chance of being implemented in the current workflow of the hospital. The concept workflow consists of the following steps (see Figure 3 for schematic workflow) [41]:

- The acquisition of the patient's anatomy using a 3D scanner. Making a scan in 1-2 minutes.
- Followed by manipulation of the scanned data in a virtual environment to create a digital cast. This process takes about 1.5 – 2.5 hours.
    - Pre-processing for the algorithm
    - An algorithm that creates the cast
- The next phase is printing the cast. Printing the cast takes the longest time, it takes about 24 - 48 hours.
- Grinding and removal of unnecessary parts, smoothing of edges to prevent pressure sores (sanding is done with 120 and 240 grit sanding paper). This takes about 30 minutes up to 1 hour.
- Verifying and checking the fit of the orthosis. Fitting the cast to the patient takes about 1 – 2 minutes.

This workflow will be tested in the pilot study.

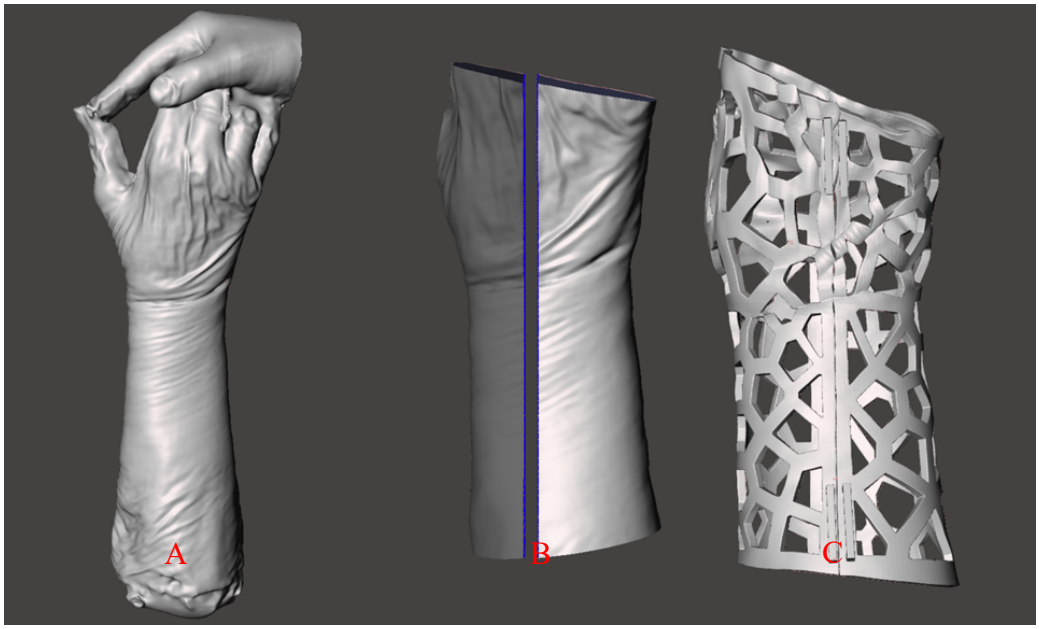

Figure 3: Schematic workflow. A) the 3D scan of the arm, B) the data is altered and prepared for the algorithm, C) the algorithm has created a cast.

Scanning the arm, digitalization process

3D scanning of the forearm

3D scanners are used to acquire the entire shape of the forearm. The use of 3D scanners helps in personalized designing. With plaster casts, the following complications can be present: excessive tightness and over-compression, and pain. Furthermore, in literature, pressure sores are described due to inadequate fit [23], [24]. A personalized design can prevent these complications, the 3D scanner gives a more precise and better fit.

3D scanners use non-uniformly emitted light, to convert a real-life object into data that can be used to develop the cast design, by comparing the recollected light after reflection of an object with the internal (calibrated) reference pattern [62]. The advantages of 3D scanning over imaging modalities are the lack of radiation, the portable character of the devices, and fast scanning times.

An EinScan H 3D scanner is available for the digitalization of the limb. The EinScan H is a handheld and lightweight 3D scanner with infrared light and hybrid LEDs. This scanner is suitable for body scanning, as it can correct small movements during scanning [63]. The scanner's accuracy is essential to ensure a good fit, the scanner's accuracy is 0.05 mm (product property). A semi-automated algorithm processes this data into a 3D model and is further processed.

Scanning setting

The scan is performed in Body Scan mode, with the High Detail resolution setting (resolution of 0.5 to 3 mm). The forearm is positioned horizontally in the air, with the fingers pointing upward (the arm may be supported for comfortability). The thumb and the other fingers were spread, the remaining fingers were not spread. The wrist was positioned neutrally (20-degree dorsiflexion and no sideward deviation). The scanning time is about 1-2 minutes. However, this depends on the experience of the operator and if the patient can hold the position perfectly during the scan. The scanner is held at a distance 37 and 57 cm (based on the manual) for optimal scanning. After scanning, a model is constructed.

Post-processing

After the scan data is processed, only the area of interest is selected to post-process. So excess scanning areas, such as the shoulder and upper arm, were removed from the data. The collected point cloud meshed as an unwatertight model. Finally, the mesh was exported as an STL. Then the model was loaded into Meshmixer (AutoDesk, Inc., San Rafael, USA). To create a cast, the following steps must be performed:

- The fingers and thumb are removed in Meshmixer, using the Plane Cut function with the No Fill option.
- The arm must be trimmed to the desired length of the cast using the Plane Cut function with the No Fill option.
- To allow for some swelling and prevent excessive tightness of the cast, a small offset of 0.5 mm in the normal direction was put in place, by selecting the trimmed surface and using the Offset function.
- The model is divided into two parts, a radial, and an ulnar part, using the Split function.
- Export and save of both parts.

Cast creation algorithm

The shape (contours) of the cast is created. The following step is constructing the cast its thickness and pattern. This is achieved with a semi-automated algorithm in Rhino 6 (Rhinoceros, Seattle, WA, USA) with the addition of RhinoResurf (Trunhoo Network Technology, Nanjing, Jiangsu, China), Grasshopper, and Grasshopper LunchBox plugins.

The model, which is the result of scanning, is a collection of points in space. Each point has its own X, Y, and Z coordinate. All these points together form a 3D model. The total surface of the model exists out of surfaces of three cloud points, which are triangles (this is called a mesh, which is a representation of three close points that forms a triangle). So now the model has points and a surface connected by points. This is needed to transfer the model into a non-uniform rational basis spline (NURBS) model (NURBS are chosen while it is more accurate compared to polygons). The model is resolution independent and represented mathematically, making it a more accurate representation of the forearm. The conversion into NURBS surface of the cast is achieved with the RsMesh2Surf function from the RhinoResurf plugin.

The second step is creating a UV curve (which is a representation of the model folded out as a flat object), with the CreateUVCrv function. This function is used to measure the dimensions of the model, which are needed for pattern generation. The NURBS surfaces and the UV curves/dimensions are the input for the cast algorithm (in grasshopper). The inputs are the NURBS surfaces and the UV curves. The algorithm established the boundaries of the cast, an offset of 5 mm is created at the border of the UV curve and around the thumbhole, as these areas need to be solid. Then the algorithm makes the pattern in the UV curves. Random points are used as midpoints for the Voronoi cells, which are scaled with a factor 0.70 to ensure the ribs between the cells have a width of about 5 mm. The number of Voronoi cells is determined based on the area of the UV curve. For every 400 mm^2 a cell is added. The pattern and the borders are combined in 2D, followed by a conversion back into meshes.

The thickness is set to 3 – 4 mm, which is similar to the thickness of plaster [35], [36], [64]. The thickness of the cast is important for the immobilizing properties however, it is also important to consider a feasible workflow. Therefore, the thickness should be chosen to make a 3D printed cast in 24-48 hours and should have the perfect immobilizing properties. After this, the 3D design of the cast can be completed and exported as STL files.

Addition of the closing mechanism

Plaster casts are circularly wrapped around the forearm. This is not achievable with 3D printed materials (except for 3D printed material, which allows for thermoforming (folding)). However, this process is not comfortable for the patient. Therefore, this material is not an option. The material used in this study is solid and not foldable after printing, so it is not possible to fold it around the arm.

The 3D-printed cast is fitted to the forearm after it is printed. Therefore, the printed cast should consist of two parts with a closing mechanism. The two parts must be held together, this is done with Velcro® fasteners (Velcrotex SATM, Assens, Switzerland). Velcro straps are chosen due to their availability and multi-functionality, costs, and because the straps can be loosened or tightened if necessary (excessive tightness, caused by swelling or reduced swelling). The arcs are designed in Tinkercad (AutoDesk, Inc., San Rafael, USA) and placed onto the cast in Meshmixer at the proximal end of the cast and at the wrist area. The straps go through the arcs. These arcs ensure that the straps will be fixated at the right place. A total of eight arcs are placed. Then the ulnar part and the radial part are combined and exported, and the design is ready to print.

Materials

Many 3D-printed casts or splint designs have emerged in the past years, each with its specific design and choice of material, of which several examples include Xkelet, ActivArmor, and Castprint. There is no consensus on which material has the optimal qualities to be used for an orthosis. Further, whether these casts could withstand the forces while keeping the fracture immobilized remains unknown, no scientific proof of effectiveness is available. The aim of the current study is to investigate which material is best for 3D-printed casts.

The most important condition is that the material immobilizes the fracture (the material is one of the components to immobilize the fracture using a cast). Immobilization ensures some pain relief for the patient and correct healing [31]. The material properties are one of the components which determine the effectiveness of the 3D-printed cast. Theoretically, the material of an orthosis should have several qualities, including high stiffness and a high Young's modulus. Young's modulus (E) is the resistance against deformation when a force is applied. There is a positive linear relationship between the E and the stiffness of the material. This is important because if the material is easily deformed, there is a chance of inefficient fracture healing due to a change in the shape and fit of the cast [65]. Also, the ultimate strength should be as high as possible to prevent the cast from breaking, whether due to external forces such as bumping the cast or internal forces such as force generation of the wrist. Additionally, it is important to know the failure mechanisms of the materials under flexural and tensile forces since fragmentation can lead to sharp edges, which is unfavorable. The material should not be too brittle to prevent cuts in case of breakage of the cast.

Other important conditions include safety and costs. All materials should not be cytotoxic or give skin reactions. In addition, they should be water-resistant. This will provide better hygiene and improved activity of daily living for the patient [38]. The material is only suitable for medical production if those conditions are fulfilled, according to ISO 10993-1 [66]. Furthermore, the printing time is important in choosing the right material.

Selection of materials

We selected materials for FDM printing based on the materials that previously have been described for 3D casts or braces. The most mentioned material is polylactic acid (PLA) [42], [43]. PLA is easy to use in 3D printers, lighter than plaster, and biocompatible as PLA is used for a wide range of applications: suture threads, bone fixation screws (however, it is not certified). [42]. Górski *et al.* compared different materials for the casts and marked PLA as the most favorable based on strength, accuracy, favorable costs, biocompatibility, and recyclability. [42] Another option is to explore the use of a compound material constructed out of PLA and polyhydroxyalkanoate (PHA). A possible advantage of adding PHA is a reduction of the brittleness of the material. Other possible materials included co-polyester (CPE) and polyethylene terephthalate glycol-modified (PETG; this filament is named Guideline, a medical grade ISO 10993 FDA registered material) based filament. Based on the requirements of the cast, the previous literature, and the advice of 3D-printing specialists (Ultimaker) a total of 5 materials of interest will be tested, including PLA, Tough PLA, PLA-PHA, CPE, and Guiline filament. All these materials could be used in the production of orthosis and braces, as they are easy to print, are recyclable, and have the same range of strength as plaster or better. Based on material characteristics from the test, one material is selected for the cadaver study.

Method for testing the materials properties

The materials will be subject to tensile and flexural testing. These tests are conducted following the ISO standards, ISO 178 and ISO 527, respectively. The procedures will be explained in detail below.

Tensile strength setup and testing

Tensile testing was performed with a Zwick retrofit 1445 retroline (ZwickRoell, Georgia, USA). The test setup is shown in Figure 4a. Test samples were clamped into the grips that were spaced 130 mm apart. A pretension was set at 5N to prevent a curved region at the start of the stress/strain diagram. The test was initiated when pretension levels were reached. The test speed was set to a constant rate of 1 mm/min. During testing, the applied force (N) was measured, as well as the displacement between the grips (mm), with a sampling rate of 10 Hz. The test ended when the sample broke or when the elongation was 15 mm, since this the test would take too much time. The failure mechanism of each sample was noted. Three measurements of tensile strength were obtained during the test, including maximum tensile strength, breaking strength, and tensile modulus. With this test the following parameters were determined:

Tensile formulas

Tensile stress

$$\sigma_t = \frac{\mathrm{F}}{\mathrm{A}};\ \sigma_t = Tensile\ stress\ in\ MPa, F = applied\ force\ in\ N, A = test\ sample\ crosssectional\ area\ in\ mm^2$$

Tensile strain

$$\varepsilon_t = \frac{\Delta\ \mathrm{L}}{L_0}\%;\ \varepsilon_t = tensile\ strain\ in\ \%, \Delta\ \mathrm{L} = \text{Increase of gripping distance (distance between two supports) in mm}, L_0 = intial\ gripping\ distance\ in\ mm$$

Tensile modulus

$$E_t = \frac{\sigma_{t2} - \sigma_{t1}}{\varepsilon_{t2} - \varepsilon_{t1}};\ E_t = Tensile\ modulus\ in\ MPa, \sigma_{t1,2} = Tensile\ stress\ corresponding\ to\ \varepsilon_{t1,2}\ in\ MPa, \varepsilon_{t1,2} = tensile\ strain\ 1{,}2\ in\ \%\ (\varepsilon_{t1} = 0.05\%\ \&\ \varepsilon_{t2} = 0.025\%)$$

Flexural testing setup

Flexural testing was performed with a Zwick Z5.0 (ZwickRoell, Georgia, USA) machine. The test set-up is shown in Figure 4b. Test samples were placed on two supports with a radius of 5.0 mm and the span was set to 64 mm. A pretension was set at 5N to prevent a curved region at the start of the stress/strain diagram. The radius of the loading edge was 5.0 mm and loading was applied at mid-span. After reaching the pretension, the test was started. The test speed was set to a constant rate of 2 mm/min. During testing, the applied force (N) was measured, as well as the deflection at mid-span (mm), with a sampling rate of 20 Hz. The test ended when the sample broke, or a deflection of 15 mm was reached, since a deflection of more than 15 mm would not be representative for flexural modulus and strength calculations, because of the influence of shear forces, according to Timoschenko's beam theory [67]. The failure mechanism of each sample was noted.

Flexural strength testing

The Flexural testing will provide us the measurement of the following variables: the maximum bending force, the breaking strength, the yield strength (the yield strength is calculated by finding the between the stress-strain curve and the flexural modulus slope with a 0.2% offset), and the Elastic modulus. The elastic modulus is calculated with the following formulas.

Flexural formulas

Flexural stress

$$\sigma_f = \frac{3\,\mathrm{F}\,\mathrm{L}}{2\,\mathrm{b}\,h^2};\ \sigma_f = flexural\ stress\ in\ MPa, F = applied\ force\ in\ N, L = span\ in\ mm, b = test\ sample\ width\ in\ mm, h = thickness\ of\ the\ test\ sample\ in\ mm$$

Flexural modulus

$$E_f = \frac{L^3\,P}{48\,l\,\mathrm{dx}}; L = span\ width\ in\ mm, P = gradient\ (i.e., slope) of\ the\ load\ deflection\ curve\ in \frac{N}{mm}, l = moment\ of\ inertia\ in\ M, dx = deflection\ in\ mm.$$

Test samples

The test samples have certain dimensions for the tests according to the corresponding ISO standards, ISO 178 and ISO 527, respectively. The dimensions for the flexural test samples and tensile test samples are presented in Table 3 and the image is shown in Figure 5[1,2].

The design was exported as a standard tessellation language (STL) file imported into Ultimaker Cura (Ultimaker B.V., Utrecht, Netherlands). All samples were oriented vertically (Z-axis, see Figure 6) and horizontally (on XY plane, see Figure 6) placed onto the build platform. Then the variables could be tested for the influence of the different printing directions. The setting in Cura were as follows: Infill density was set to 20%, with an infill pattern triangle, support density was set to 20%, the support material was polyvinylalkohol (PVA, which dissolves with water) and layer thickness to 0.2 mm. Further settings were set to default. For both the flexural and tensile tests, seven samples for each printing direction were printed per material. Six of the samples were used for testing and one was used as a back-up, in case a test failed. In total, 35 samples were printed for flexural testing and 35 samples were printed for tensile testing. Before testing, the sample width and thickness were checked at the mid-length of the specimen with a caliper (Mitutoyo, Kawasaki, Japan) for compliance with the design dimensions. If the deviation was more than 5% percent of the original dimension, then the samples were excluded for testing. However, none of the printed samples had a deviation larger than 0.5 mm.

Table 3: Dimension of the test samples

Dimensions in mm

		Flexural test samples	Tensile test samples
Length	*Overall*	80.0	170.0
	Narrow portion		80.0
Width	*Overall*	10.0	20.0
	Narrow portion		10.0
Thickness	*Overall*	4.0	4.0

[1] ISO 527. Plastics – Determination of tensile properties. 2019.
[2] ISO 178. Plastics – Determination of flexural properties. 2019.

Figure 4: A) Zwick retrofit 1445 retroline, B) Zwick Z5.0

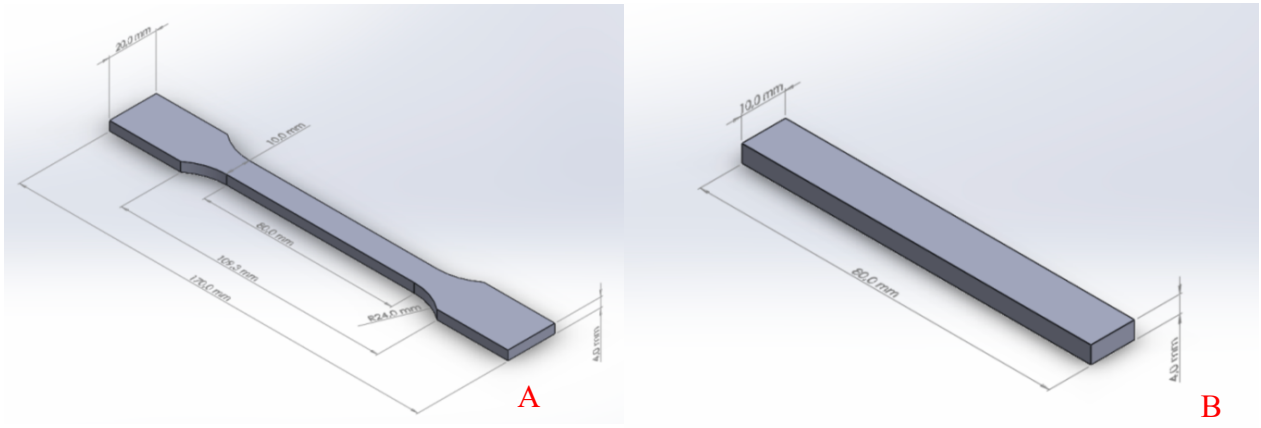

Figure 5: dimensions of the samples A) tensile strength testing and B) flexural strength testing

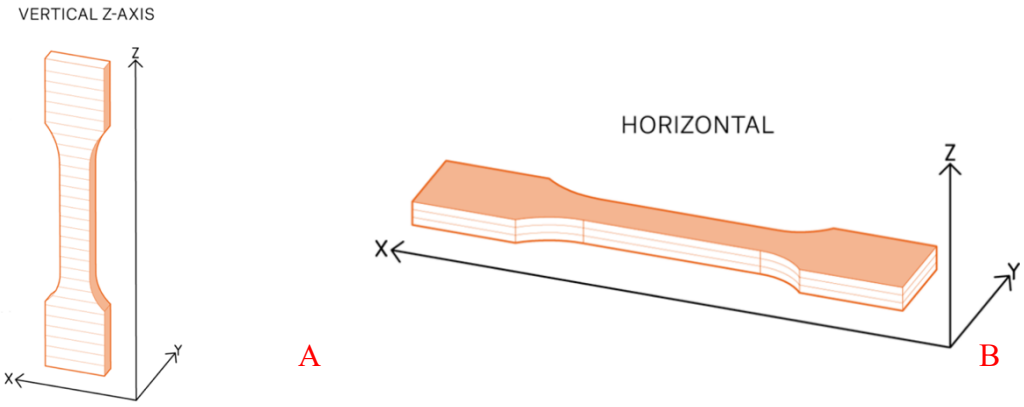

Figure 6: Orientation of the printed samples. A) Sample printed in the vertical Z-axis, B) sample printed horizontally in XY plane.

Statistical analysis

Data calculations were performed in Microsoft Excel (Microsoft, Redmond, WA, USA) and MATLAB R2021b (The MathWorks Inc., Natick, MA, USA). These outcomes were used for the statistical analysis with SPSS Statistics Version 28 (IBM, Armonk, NY, USA).

The mean value for each parameter, per printing direction per material, was calculated. To determine if the mean values differ significantly, a Multivariate one-way Analysis of Variance (MANOVA) was performed. A Bonferroni post hoc test was performed to determine which materials differed significantly. Bonferroni was used to correct the error rate when using MANOVA. During statistical analysis, a significance level of $p = 0.0014$(0.05/35, there were 35 comparisons) was used.

Lastly, the material parameters were ranked from one to five. The first material implicates the best material, five the worst for the use for printing 3D wrist casts. For the calculated parameters, the lowest value was always the most favorable. When no significant difference could be found between materials, the ranking was adjusted to 1 to 5, 1 to 4, and so on. The lowest-scoring material was chosen to use as the material for the 3D-printed wrist casts.

Results

For all the samples, during both the tensile- and flexural testing, the cracked samples showed minimal delamination. The minimal delamination did not result in sharp edges, which could be harmful for the patients.

In Table 4, the descriptive statistics of the tested parameters are presented. For all parameters, the ANOVA showed a significant difference between the material groups ($p = 0.001$). Post-hoc analyses were performed to pinpoint the material with the best properties for all parameters (Tables 5.1 and 5.2).

For all parameters, the lowest score in the system would theoretically implicate the material with the best qualities (see Table 6 for the result). All parameters together resulted in the best score for PLA. Therefore, PLA is selected to be the material to produce the 3D-printed wrist casts in de human cadaver study.

Table 4: Mean descriptive of the parameters

		Maximum Bending Force in N	*SD*	*Force at Break at N*	*SD*	*E modulus in Mpa*	*SD*	*Yield Strength in N*	*SD*	*Maximum Tensile force in N*	*SD*	*Force at Break in N*	*SD*	*Tensile modulus in Mpa*	*SD*
T PLA	X Y	93,2	3,9	90,2	4,4	801,5	26,1	62,0	1,8	949,1	41,6	925,4	37,5	2046,9	317,0
	Z	112,3	1,3	-	-	808,8	10,1	54,8	0,4	1239,4	16,9	948,2	61,6	2180,5	65,3
PLA	X Y	75,5	8,8	75,2	8,8	932,3	40,8	43,2	1,5	918,9	71,8	904,2	80,9	2627,9	47,4
	Z	120,8	1,4	111,5	5,3	902,0	11,0	79,9	1,0	1125,2	15,0	1114,4	16,9	2113,5	55,4
PLAPHA	X Y	88,8	7,9	88,5	7,7	876,9	51,0	45,2	2,3	844,6	108,2	828,0	110,5	2653,9	41,2
	Z	119,3	2,8	94,5	11,0	847,4	17,1	75,3	1,2	1193,0	13,8	1164,1	18,9	2114,9	34,5
CPE	X Y	37,3	6,0	36,6	5,9	492,0	17,0	11,5	0,8	331,0	84,2	326,1	84,7	1365,0	92,4
	Z	96,9	6,8	-	-	559,9	28,9	41,3	2,1	1207,2	15,1	1012,0	56,3	1455,2	35,7
ETG	X Y	67,7	10,6	66,6	10,3	562,8	21,9	43,1	2,1	857,2	86,0	834,2	91,1	1546,4	53,5
	Z	90,7	3,4	-	-	511,8	10,9	40,3	2,8	1010,5	12,1	673,8	235,6	1329,4	16,9

Table 5.1: P-values of Bonferroni post hoc test for the Vertical-Z samples.

MAXIMUM BENDING FORCE IN N		TPLA	PLA	PLAPHA	CPE	PETG
	TPLA	-				
	PLA	0.0019	-			
	PLAPHA	1.0000	0.0331	-		
	CPE	**0.0001**	**0.0001**	**0.0001**	-	
	PETG	**0.0001**	0.7068	**0.0002**	**0.0001**	-
FORCE AT BREAK AT N		TPLA	PLA	PLAPHA	CPE	PETG
	TPLA	-				
	PLA	0.0096	-			
	PLAPHA	1.0000	0.0297	-		
	CPE	**0.0001**	**0.0001**	**0.0001**	-	
	PETG	**0.0001**	0.4625	**0.0001**	**0.0001**	-
E-MODULUS IN MPA		TPLA	PLA	PLAPHA	CPE	PETG
	TPLA	-				
	PLA	**0.0001**	-			
	PLAPHA	0.0024	0.0456	-		
	CPE	**0.0001**	**0.0001**	**0.0001**	-	
	PETG	**0.0001**	**0.0001**	**0.0001**	0.0048	-
YIELD STRENGTH IN N		TPLA	PLA	PLAPHA	CPE	PETG
	TPLA	-				
	PLA	**0.0001**	-			
	PLAPHA	**0.0001**	0.3730	-		
	CPE	**0.0001**	**0.0001**	**0.0001**	-	
	PETG	**0.0001**	1.0000	0.3639	**0.0001**	-
MAXIMUM TENSILE FORCE IN N		TPLA	PLA	PLAPHA	CPE	PETG
	TPLA	-				
	PLA	1.0000	-			
	PLAPHA	0.2327	1.0000	-		
	CPE	**0.0001**	**0.0001**	**0.0001**	-	
	PETG	0.5226	1.0000	1.0000	**0.0001**	-
FORCE AT BREAK IN N		TPLA	PLA	PLAPHA	CPE	PETG
	TPLA	-				
	PLA	1.0000	-			
	PLAPHA	0.3941	1.0000	-		
	CPE	**0.0001**	**0.0001**	**0.0001**	-	
	PETG	0.6186	1.0000	1.0000	**0.0001**	-
TENSILE MODULUS IN MPA		TPLA	PLA	PLAPHA	CPE	PETG
	TPLA	-				
	PLA	**0.0001**	-			
	PLAPHA	**0.0001**	1.0000	-		
	CPE	**0.0001**	**0.0001**	**0.0001**	-	
	PETG	**0.0001**	**0.0001**	**0.0001**	0.3626	-

Table 5.2: P-values of Bonferroni post hoc test for the horizontally printed samples

MAXIMUM BENDING FORCE IN N		TPLA	PLA	PLAPHA	CPE	PETG
	TPLA	-				
	PLA	0.0018	-			
	PLAPHA	0.0143	1.0000	-		
	CPE	**0.0001**	**0.0001**	**0.0001**	-	
	PETG	**0.0001**	**0.0001**	**0.0001**	0.0421	-
FORCE AT BREAK AT N		TPLA	PLA	PLAPHA	CPE	PETG
	TPLA	-				
	PLA	**0.0001**	-			
	PLAPHA	**0.0001**	**0.0001**	-		
	CPE	1.0000	**0.0001**	**0.0001**	-	
	PETG	1.0000	**0.0001**	**0.0001**	1.0000	-
E-MODULUS IN MPA		TPLA	PLA	PLAPHA	CPE	PETG
	TPLA	-				
	PLA	**0.0001**	-			
	PLAPHA	0.0021	**0.0001**	-		
	CPE	**0.0001**	**0.0001**	**0.0001**	-	
	PETG	**0.0001**	**0.0001**	**0.0001**	**0.0001**	-
YIELD STRENGTH IN N		TPLA	PLA	PLAPHA	CPE	PETG
	TPLA	-				
	PLA	**0.0001**	-			
	PLAPHA	**0.0001**	**0.0001**	-		
	CPE	**0.0001**	**0.0001**	**0.0001**	-	
	PETG	**0.0001**	**0.0003**	**0.0003**	1.0000	-
MAXIMUM TENSILE FORCE IN N		TPLA	PLA	PLAPHA	CPE	PETG
	TPLA	-				
	PLA	**0.0001**	-			
	PLAPHA	**0.0001**	**0.0001**	-		
	CPE	0.0028	**0.0001**	0.8112	-	
	PETG	**0.0001**	**0.0001**	**0.0001**	**0.0001**	-
FORCE AT BREAK IN N		TPLA	PLA	PLAPHA	CPE	PETG
	TPLA	-				
	PLA	0.0956	-			
	PLAPHA	0.0114	1.0000	-		
	CPE	1.0000	0.9859	0.1680	-	
	PETG	**0.0008**	**0.0001**	**0.0001**	**0.0001**	-
TENSILE MODULUS IN MPA		TPLA	PLA	PLAPHA	CPE	PETG
	TPLA	-				
	PLA	0.0901	-			
	PLAPHA	0.1045	1.0000	-		
	CPE	**0.0001**	**0.0001**	**0.0001**	-	
	PETG	**0.0001**	**0.0001**	**0.0001**	**0.0001**	-

Table 6: Scoring system

		TPLA	PLAPHA	PLA	CPE	PETG
Maximum Bending Force	Z	1	1	1	3	2
	XY	1	1	1	2	3
Force at Break	Z	1	1	1	3	2
	XY	1	3	**2**	1	1
E-modulus	Z	2	2	1	3	3
	XY	2	2	1	3	4
Yield Strength	Z	1	2	**2**	3	2
	XY	3	2	1	4	4
Maximum Tensile force	Z	1	1	1	2	1
	XY	1	1	**2**	1	3
Force at Break	Z	1	1	1	2	1
	XY	1	1	1	1	2
Tensile modulus	Z	2	1	1	3	3
	XY	1	1	1	2	2
Costs		2	1	1	3	4
Printing speed		3	1	1	2	3
Total score		24	22	19	38	40

Discussion

This study investigates the integrity of various 3D printing materials that might be suitable to produce casts for the immobilization of DRFs. PLA, produced by Ultimaker, was considered the best based on the scoring system. The samples were printed in two different orientations to gain a more complete overview of the material behavior. This gave more adequate meaning to the strength values and helped in the printing orientation for the 3D printing of the wrist casts.

The most suitable material should score the best for both directions combined, as both printing directions will be present in the printed cast. In Tables 4.1 and 4.2, the Bonferroni post hoc test for the Vertical-Z and horizontally XY plane samples showed which parameters differ significantly. The materials were scored for each parameter per direction, this is shown in Table 5. PLA scores best for all parameters except for force at break-, maximum tensile force in the printed in the XY plane, and yield strength in the vertical z-axis printed direction. Even though PLA scored less good for these parameters, for these parameters, PLA came in second. However, the materials that scored better than PLA for one direction scored worse in the other direction than the parameters where PLA scored less. Therefore, PLA is the best material as it scored best, in printing both the XY plane and vertical z-axis direction. PLAPHA came in with a close second place, followed by TPLA. CPE and PETG scored almost twice as high compared to the others, making these materials the least suitable.

Only a limited number of studies have been published about material properties. The manufacturers do test their own materials. However, properties of the tensile strength, tensile modulus and flexural modulus in different printing directions are not reported in the open literature or when reported not compared to other materials. Several practical explanations exist for this lack of comparison in literature, including widely different printers, printer settings, and tests. To allow for an accurate comparison of each material printed in different directions, the tests were repeated with the same conditions for each material. It is peculiar the result showed that PLA was better than TPLA, while TLPA is PLA strengthened with additional additives. TPLA scored in three things better than PLA. First, it was better in the vertical Z-axis for Yield strength. Secondly, TPLA was better in the XY plane for the force at the Break for the Flexural test. Lastly, TPLA was better for Maximum Tensile Force printed in the XY plane. However, these higher values did not show that TPLA was better than PLA overall.

The printer settings were the same for all materials. However, there were some differences, as the material settings were specific for each material. Two of the specific settings are the temperature and printing speed. TPLA is printed slower than PLA otherwise, the material was not extruded. This could be that either the material clogs up the nozzle and the material can get burned, or the material is too fluid and is spread out more than it should be, which could result in a less optimal strength.

The materials were selected based on the advice of filament manufacturers and the advice of 3D-printing specialists (Ultimaker), and based on the literature focused on printed orthosis for wrist fractures. Ultimaker provides printing materials (PLA, TPLA, CPE) and technical support. The other materials (CPE, Guideline(PETG)) were bought from other retailers. The materials were tested independently. In this study, the material selection was limited to the materials that were printable on an Ultimaker S5 (Ultimaker BV, Geldermalsen, the Netherlands) with 2.85 mm nozzle size and print temperature limit of 280°. To the knowledge of the author, these materials are most suitable for the cast researched in this study. The possibility exists that there are other materials suitable to produce 3D-printed cast for DRFs that do not fall within the scope of this study. Additionally, further research should be conducted on print settings which potentially could be improved. Furthermore, new materials and 3D printers become available, making it essential to continue research to test new potential materials and 3D-printers.

During the tests, delamination was observed in the samples, this can be caused by small air pockets between the layers due to the temperature differences while printing. This delamination did not result in sharp edges, which is desirable.

Conclusion

PLA is the most suitable material to produce 3D-printed wrist casts, based on flexural and tensile material parameters, as well as printing costs and time.

Cadaver study

Introduction

The Colles fracture is one of the most treated distal radius fractures [68]. This is classified as the extra-articular 2R3-A2.2 fracture by the AO. This fracture will be simulated. This is an injury with a transverse fracture of the radius just above the wrist (20–35 mm proximal to the articular surface; the radio-carpal joint), with dorsal displacement of the distal fragment. It is more common in older people, and the fracture is often caused by a fall on an outstretched hand (FOOSH, the in hand is positioned in extension) [12], [14].

Stable Colles fractures are treated with closed reduction and cast immobilization [15]. The cast extends from below the elbow to the metacarpal heads and holds the wrist somewhat flexed and in ulnar deviation. [69]

Treatment with plaster cast

A plaster cast is placed on the wrist to relieve pain and to hold the anatomical position of the bones for 3-6 weeks. In case of a stable non-displaced fracture, plaster for one week is sufficient for pain relief [18], [19]. Plaster casting is cheap and reliable for immobilizing the fracture. However, there are disadvantages. Plaster is not waterproof, it can give pressure sores and is associated with compartment syndrome (plaster is applied when swelling is present. Therefore, the cast could be too tight) [22], [23]. Further, it lacks the possibility of visual inspection of the skin, impairs cleaning and ventilation of the arm, and can lead to hygiene problems caused by increased perspiring, itching. [19], [21] Another disadvantage of plaster casts is the weight, which is approximately 500 gram [28]. This can make it uncomfortable for the patient. It can cause pain (in the neck or back), muscle loss, a decrease muscle in strength [29], [70], and temporary inactivity can also result in a decreased optimal healing process and stiffness. Up to 30% of the patients experience complications. [23], [24]. The preferred cast is an above-the-elbow cast. However, a forearm cast is sufficient. [71]–[73]

An alternative to plaster treatment is customized 3D-printed orthoses. [28]. 3D-printed orthoses could solve some of the problems associated with plaster [19], [21], [26], [28]. A pilot study performed in our hospital has shown that it is feasible to print 3D casts in the hospital. The pilot study was conducted in patients with greenstick and torus/buckle fractures. The aim of the current study is to characterize the magnitude of fracture displacement during static load in human cadaver models with Colles fractures. Since standard mechanical testing, using a 3-point bending set-up, does not consider soft tissue displacement, a test setup must be developed. Furthermore, a workflow must be designed to simulate the Colles (AO; 2R3-A2.2) fractures.

Method

3D casts

3D scans of the forearm

A total of ten human arms were used in the current study. These arms were obtained from the University Medical centrum of Utrecht, informed consent was given prior to their death.

These ten arms were scanned with the EinScan H 3D scanner. According to the EinScan H 3D scanner methodology, the scan was performed in Body Scan mode with the High Detail resolution setting. The scan will be made with the forearm positioned on a platform with a pin on which the arm is fixated, the thumb and the other fingers were spread by a second person. The wrist was positioned neutrally (20-degree dorsiflexion and no sideward deviation). After scanning, a model is constructed.

Design of the cast

After the 3D model was constructed, only the data of the forearm is used for post-processing (see Figure 7A) the total scan, 7B) the image of the forearm as base for the design). The data was exported as an STL. Then the model was loaded into Meshmixer (AutoDesk, Inc., San Rafael, USA). To create a cast the following steps were performed:

- In Meshmixer, the fingers and thumb were removed in the designing phase using the Plane Cut function with the No Fill option.
- The arm was trimmed to the desired length of the cast using the Plane Cut function with the No Fill option.
- To allow for some swelling and prevent excessive tightness of the cast, a small offset of 0.5 mm in the normal direction was used, by selecting the trimmed surface and using the Offset function.
- The model is divided into two parts, a radial and an ulnar part, using the Split function.
- Export both parts as STL.

The shape of the cast is created, now its pattern and thickness must be created. This is achieved with a semi-automated algorithm in Rhino 6 (Rhinoceros, Seattle, WA, USA) with the addition of RhinoResurf (Trunhoo Network Technology, Nanjing, Jiangsu, China), Grasshopper, and Grasshopper LunchBox plugins. The cast can be seen in Figure 7C. The mechanism is described in the technical background section. The last step in the designing phase is to add the closing mechanism. Now the cast is created and ready for printing.

Printing the 3D casts

The designs are printed with the Ultimaker S5. Based on the material study, the 3D-printed wrist casts were made with PLA. The settings for all the casts were the same. The layer thickness was set to 0.2 mm with PVA as support material (which dissolves in water after printing), and the casts were orientated upward.

After printing, the casts were fitted before the cantilever test was conducted. In case the cast did not fit perfectly, the cast was excluded. An exclusion criterion of a loose fit, defined as >1 cm space between the hand and the cast, was used.

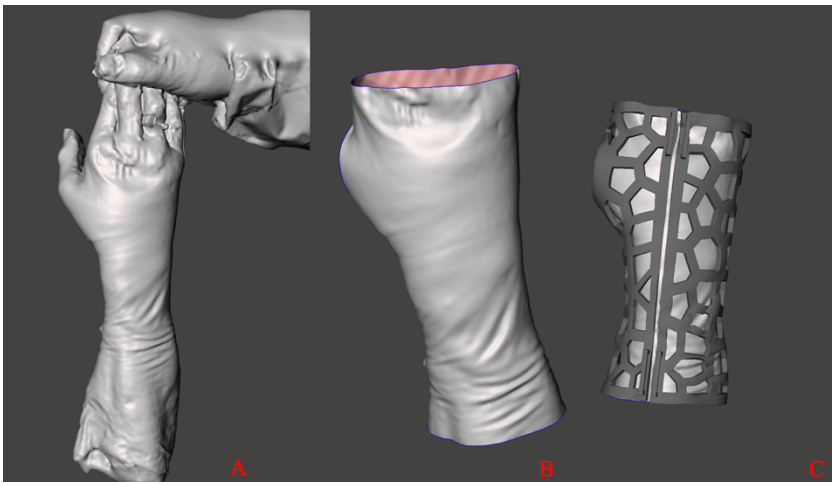

Figure 7: A) The scan of the arm, B) the base for the design process, C) the 3D cast placed on the arm.

Simulation of fractures

Designing phase guides

This study will focus on the extra-articular 2R3-A2.2 fracture, which is a Colles fracture. This fracture will be simulated, a workflow is designed to simulate the fractures in the same way in the ten cadaver samples. Therefore, surgical cutting guides are used. These guides ensure the reproducibility of each fracture. Before a surgical guide could be designed, CT scans were made of all the arms (Philips Brilliance iCT, 256 slice CT (Royal Philips N.V., Eindhoven, the Netherlands) with a slice thickness of 0.625 mm, CT settings of 120 kV and 30mA, voxel size of 0.98 mm). Based on these scans, the surgical guides are produced as follows (see Figure 8 and 9):

- Exporting CT scans into Philips Intellispace Portal (PIP) (Royal Philips N.V., Eindhoven, the Netherlands) and 3D rendering the slices.
- Segmentation of the radius PIP.
    - Image processing with Autodesk Meshmixer (version 3.5.474 for Mac ©2017, Autodesk, Inc. San Rafael, CA, USA)
    - Make a base plate so that the guide fits onto the distal end of the radius, using the function Select for the selection of area. This area is extruded with 2 mm to form the base plate of the surgical guide.
    - Create incision/hole(s) into the guide. The location of the incision/hole(s) needs to be aligned so that AO 23-A2.2 fracture can be simulated.
        - Based on the AO classification, the angle in a Colles fracture was measured and used as standard. The angle based on the image of the AO classification is twenty degrees, this was used to simulate the fracture line.
        - The cutting line was set near the tubercle of Lister, this was done as this is a reliable orientation point to place the guide.
        - Create 2 mm holes for K-wires to fixate the guide onto the radius.
        - A number which corresponds to the arm is placed on the surgical cutting guide so the correct guide can be matched to the arm.
- After the design is accomplished, the surgical guide is printed with Form 3 (Formlabs Inc., Somerville, MA, USA), color resin (0.1 mm layer thickness).

The surgical guides are checked if the fit is achieved. This is done by fitting the guides on 3D-printed anatomical models of the radii of the ten forearms (see Figure 8C).

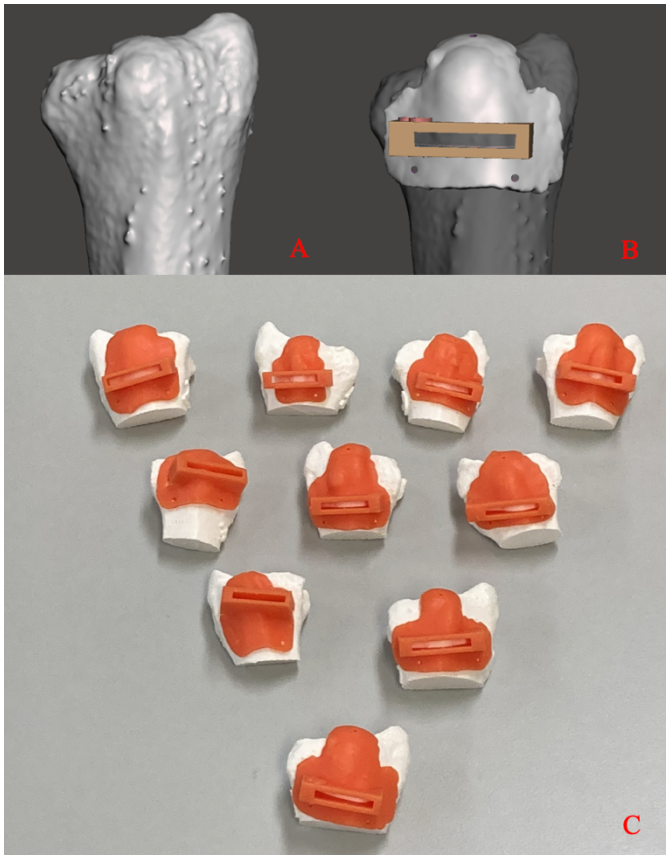

Figure 8: A) The segmented Radius, B) The surgical guide placed onto the Radius, C) The surgical guides fitted onto the 3D-printed proximal radius for control.

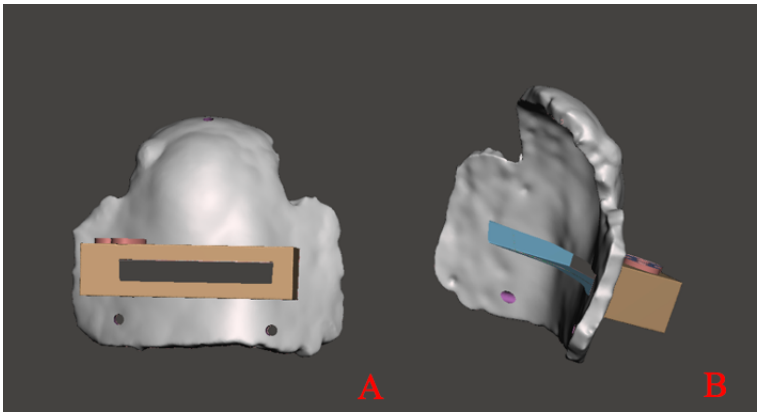

Figure 9: A) front view of the surgical cutting guide, B) side view of the surgical cutting guide, here can be seen that the slit is a trapezium shape which will allow for cutting through the whole width of the Radius.

Appling the guides

The guides are produced and verified on the 3D-printed proximal radii. The following step is to simulate the fractures. This is achieved in a few steps (see Figure 10):

- Determine the dorsal side of the arm;
- Find the tubercle of Lister (dorso-radial area of the wrist);
- Make an incision of 5 cm above the lister, perpendicular to the arm's length.

- Detach the remaining tissue between the skin and the bone. First the skin (epidermis, dermis, and the subcutaneous tissue), antebrachial facia, then the extensor retinaculum, and then between the tendon sheaths of the extensor carpi radialis brevis and the extensor pollicus longus, Lister's tubercle can be found. The tissue is made loose and set aside from the bone to fit the surgical cutting guide. The detachment is as least as possible to maintain the integrity and strength of the forearm.
- Place and fit the guide onto the radius.
- Use an osteotome and hammer to simulate the fracture.

Test setup

Cantilever test

The goal is to measure the immobilization properties of the cast. The most common and conventional way to measure stiffness is the three-point- or four-point flexural test [74]. Although this is a consistent and reliable method, it does not consider the cast's shape and design. Therefore, a different test is needed to represent a more realistic load scenario.

The stiffness is measured by a cantilever bending test (see Figure 11 and 12). The cantilever test most closely represents the realistic anatomical situation (where the loads represent normal daily activities like picking up a glass or carrying a bag) wherein a patient can move the wrist while wearing the cast. The arm and cast will be placed in an angle at which the applied force generates a moment in the fulcrum. The setup allowed for flexion, extension, radial deviation, and ulnar deviation, while a load was hung onto the hand itself. A setup was made to fixate the arm (see Figure 11 and 12. This setup has a baseplate with a pin where the arms are fixated on, a support block for the arm, and there are three different distances (7,5 cm, 10 cm and 12,5 cm) so that the arms can hang freely to place a load on.

This fixation base was placed on a table. Two arm holders were 3D-printed to make sure the arms were supported sufficiently once it was placed horizontally in the setup. One arm holder was suitable for flexion and extension loading, while the other holder was suitable for radial and ulnar loading. The Table was placed between a horizontally oriented image intensifier, Philips Zenition 70 Mobile C-arc (Philips Medical Systems International BV, Best, Netherlands) for X-ray screening of the unloaded and loaded arms. For each scan, the cadaver arm was centered as much as possible.

Workflow

First, a scan was made of the unloaded arm (lateral and AP). The next step is to place a load at the distal end, which will be increased in steps (one to four kilograms, the load will mimic the forces produced in the wrist) [75]. This was done first for flexion, followed by ulnar deviation, then extension, and at last, radial deviation. Due to the different sizes of the arms, the setup was made customizable so that the setup was proportionally equal for every direction and every arm.

Data collection

A radiographic image was made for each load and every direction. This image was loaded into Jivex Review Client (version 5.2.0.27). In this program, the angle of the fracture was measured. The mean and maximum angles were calculated with SPSS. Additionally, the angle of displacement is measured.

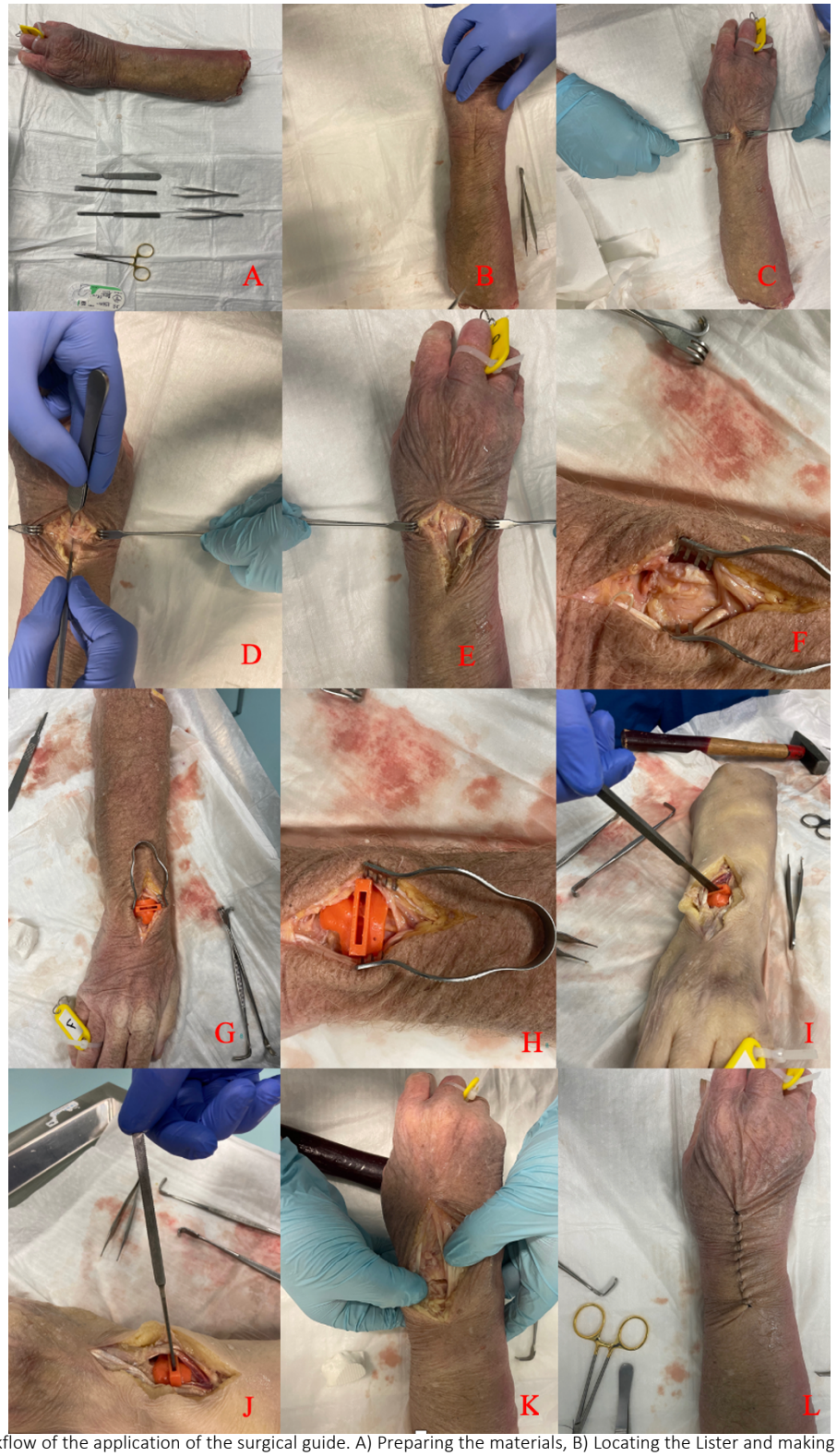

Figure 10: Workflow of the application of the surgical guide. A) Preparing the materials, B) Locating the Lister and making an incision through the skin, C-E) Dissection through, in this order: antebrachial facia, then the extensor retinaculum, F) the lister is made loose from the tissue, G-H) the surgical cutting guide is fitted onto the Radius, I-J) with the osteotome and hammer, the fracture is made, K) control if the fracture goes through the whole radius, L) the skin is sutured to regain the integrity of the skin.

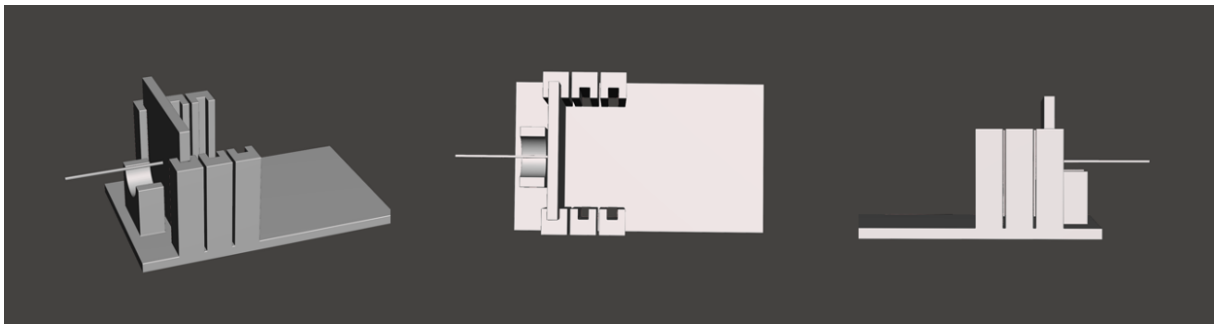

Figure 11: The test setup onto which the arms are fixated. This setup allows the investigation of loads on the casts and indirect on the fracture. The aim here is to establish if the cast's immobilization is enough to prevent secondary displacement.

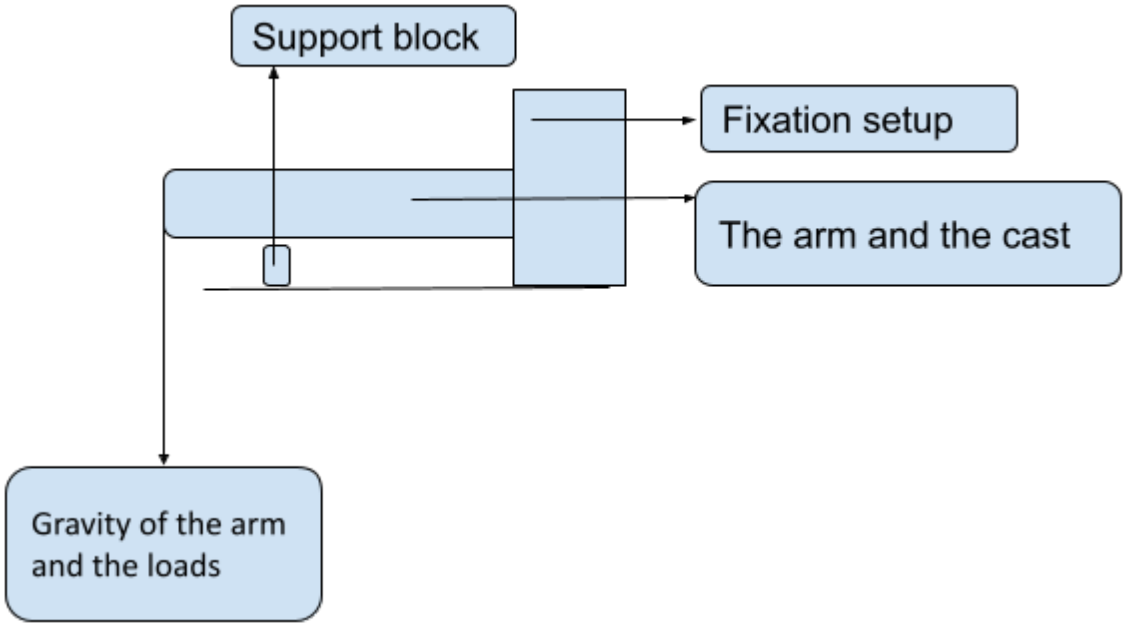

Figure 12 Schematic overview of the forces in the setup.

Results

Casts

From the ten printed casts, there were two casts where the space between the cast and wrist was more than 1 cm and therefore excluded from this study. These two casts were too loose around the wrist. The other eight casts did fit perfectly.

Data collection

Simulation of fractures

All eight remaining fractures were defined as Colles fractures based on radiographic assessment. However, the intended angle to simulate with the surgical guides were in all the cases different from the intended angle (the angle based on the AO classification was twenty degrees). This value can be found in the second column and the displacement of the radius head can be found in the third column of Table 7-9. As the angles are different in the extension and flexion direction, it means that the fracture is not made straight through the radius but there is an angle in the x-axis and the y-axis.

Three of the surgical cutting guides ruptured during the osteotome and hammer phase. It happened when the impact on the hammer caused an angular momentum that the surgical guide could not withstand.

Cantilever test

For radial deviation, no angle or displacement was measured, while in these radiographs, no displacements were visible.

In Table 7, the characteristics from the cantilever test for the flexion direction are presented. The mean fracture angle is 11.6 degrees with a mean displacement of the radius head of 4.9 degrees. For every load added, the displacement did increase. With 1 kg, the displacement increased with 1.9 degrees, for 2 kg the displacement increased with 0.5 degrees, for 3 kg the displacement increased with 0.3 degrees and for 4 kg the displacement increased with 0.1 degrees. The total mean displacement was 7.6 degrees, for the load of four kilograms.

In Table 8, the characteristics from the cantilever test for the extension direction are presented. The mean fracture angle is 16.3 degrees with a mean displacement of 5.8 degrees. For every load added, the displacement did increase. With 1 kg, the displacement increased with 0.8 degrees, for 2 kg the displacement increased with 0.8 degrees, for 3 kg the displacement increased with 0.3 degrees and for 4 kg the displacement increased with 0.5 degrees. The total mean displacement was 8.1 degrees, for the load of four kilograms.

In Table 9, the characteristics from the cantilever test for the ulnar deviation are presented. The mean fracture angle is 5.9 degrees with a mean displacement of 3.5 degrees. For every load added, the displacement did increase. With 1 kg, the displacement increased with 1.3 degrees, for 2 kg the displacement increased with 0.3 degrees, for 3 kg the displacement increased with 0.1 degrees and for 4 kg the displacement increased with 0.3 degrees. The total mean displacement was 5.5 degrees, for the load of four kilograms.

In Figure 13, a schematic representation of the radius fracture and the angle of displacement is given for a better understanding of the displacements.

Table 7: characteristics of the cantilever test for flexion

	0kg		1kg		2kg		3kg		4kg	
Arm	Fracture Angle	Displacement	Displacement	Delta	Displacement	Delta	Displacement	Delta	Displacement	Delta
1	12.9°	4.9°	7.5°	2.6°	7.5°	0.0°	8.5°	1.0°	8.5°	0.0°
2	22.7°	3.7°	8.3°	4.5°	8.3°	0.0°	8.3°	0.0°	8.3°	0.0°
3	2.2°	6.6°	6.6°	0.0°	6.6°	0.0°	6.6°	0.0°	6.6	0.0°
4	1.6°	3.6°	4.4°	0.8°	7.3°	2.9°	7.3°	0.0°	7.3°	0.0°
5	5.5°	5.0°	6.8°	1.8°	6.9°	0.1°	7.0°	0.1°	7.0°	0.0°
6	1°	3.2°	4.1°	0.9°	4.1°	0.0°	4.2°	0.1°	4.3°	0.1°
9	34°	6.7°	8.8°	2.1°	9.5°	0.7°	10.4°	0.9°	10.6°	0.2°
10	13°	5.3°	8.1°	2.8°	8.2°	0.1°	8.4°	0.2°	8.6°	0.2°

Table 8: characteristics of the cantilever test for extension

	0kg		1kg		2kg		3kg		4kg	
Arm	Fracture Angle	Displacement	Displacement	Delta	Displacement	Delta	Displacement	Delta	Displacement	Delta
1	20.9°	6.0°	6.0°	0.0°	6.0°	0.0°	6.0°	0.0°	6.0°	0.0°
2	21.8°	6.3°	0.0°	0.0°	0.0°	0.0°	0.0°	0.0°	0.0°	0.0°
3	14.8°	3.7°	6.6°	2.9°	10.0°	3.4°	10.0°	0.0°	10.0°	0.0°
4	***	***	***	***	***	***	***	***	***	***
5	9.3°	9.0°	9.0°	0.0°	9.0°	0.0°	9.0°	0.0°	9.0°	0.0°
6	4.3°	8.8°	9.1°	0.3°	11.5°	2.4°	12.7°	1.2°	16.2°	3.5°
9	39°	4.7°	6.2°	1.5°	6.5°	0.3°	6.9°	0.4°	6.9°	0.0°
10	3.9°	13.9°	15.2°	1.3°	15.7°	0.4°	16.3°	0.6°	16.5°	0.2°

*** The images were lost due to error of the C-arc.

Table 9: characteristics of the cantilever test for ulnar deviation

	0kg		1kg		2kg		3kg		4kg	
Arm	Fracture Angle	Displacement	Displacement	Delta	Displacement	Delta	Displacement	Delta	Displacement	Delta
1	1.6°	0.0°	0.0°	0.0°	0.0°	0.0°	0.0°	0.0°	0.0°	0.0°
2	5.3°	6.3°	8.4°	2.1°	8.4°	0.0°	8.4°	0.0°	8.4°	0.0°
3	4.8°	4.1°	4.2°	0.1°	5.2°	1.0°	5.2°	0.0°	6.9°	1.7°
4	13.8°	6.2°	6.3°	0.1°	6.3°	0.0°	6.3°	0.0°	6.3°	0.0°
5	7.8°	7.8°	9.1°	1.3°	9.1°	0.0°	9.1°	0.0°	9.6°	0.5°
6	7.5°	3.9°	5.7°	1.8°	5.7°	0.0°	5.7°	0.0°	5.7°	0.0°
9	2.7°	0.0°	0.0°	0.0°	0.0°	0.0°	0.0°	0.0°	0.0°	0.0°
10	3.6°	0.0°	4.6°	4.6°	5.9°	1.3°	6.6°	0.7°	6.8°	0.2°

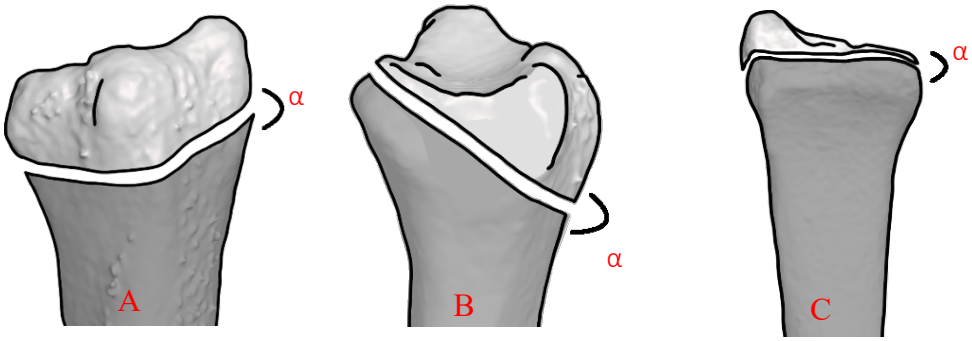

Figure 13: Schematic representation of the planned osteotomy of the distal radius. A) is the dorsal view on the distal radius, B) is the lateral view on the radius, C) is the ventral view on the radius. α represents the angle of displacement.

Discussion

The current study tries to emulate forces, comparable to static loads that are encountered in normal daily life, on human cadaver models with simulated fractures. The research question was, will there be any displacement of the fracture while a load is placed on the forearm with the cast? It is shown that there is displacement in every direction except for radial deviation with day-to-day loads. The cast supports perfectly in the radial deviation as it allows no movement, as there was no displacement visible in the radiographic images. In the results section, no table for the radial deviation was given, as no displacements were visible in the radiographic images. However, in the other directions, movement is present. This does not necessarily mean that the cast's immobilization properties are not sufficient. That remains unknown as there is no comparison to other immobilization techniques in this study. Therefore, the immobilizing properties of the cast with this design could still be sufficient for the treatment of DRFs. Furthermore, this study ignores the compensation mechanism (muscle contraction and relaxation) of the lower arm. This mechanism contributes to the stabilization of the arm and may compensate for the day-to-day loads.

The workflow to create surgical guides was feasible without the need for expensive software. Just with CT-scans, PIP, and Meshmixer, the surgical cutting guide could be created. The fractures are comparable to the fractures analyzed in Baumbach *et al.*, although they analyzed over 40.000 fractures, and this study just ten. [76]. Furthermore, the cantilever test proved to be sturdy, and efficient in switching between arms. This helped in executing the experiment within one day.

This study is the first study to investigate the immobilizing properties with a cantilever test and simulated fractures where displacement is analyzed. In Janzing *et al*., evaluation of the stabilization properties of the brace was done with an ex vivo model (which was embalmed) where a DRF fracture was simulated. [11] The fracture was simulated with the model published by Baumbach *et al.* modified: a wedge osteotomy of 10 mm dorsal/1 mm volar was made 8 mm/12 mm proximal to the dorsal/volar apex of the articular surface [11], [77]. After simulating the fractures, the arms were placed in test setup: the forearm was fixated, and a force of 20 Nm was applied to the hand, first in the dorsal and then in the radial direction. [11] Displacement was radiologically assessed, first without a brace then with a brace. The results of this study are not comparable with our study, as the setup and the loads are different. In our study, the measured displacements were smaller, which may mean that our design is more immobilizing.

In the study of Hoogervorst *et al.*, they tried to quantify the stabilizing properties of a 3D-printed short-arm cast and compare these properties with traditional fiberglass casts in a cadaveric distal radius fracture model. [56] They tested the flexion and extension of digits, pronation and supination of the hand, and 3-point bending of the arm wrapped with the cast. They only found a statistical difference for the 3-point bending test. A difference of 1 mm in absolute motion was found. [56] However, it is not clear what the clinical consequence of this motion is. The results of Hoogervorst *et al.*, showed noninferiority of the 3D-printed casts. The design of the cast in Hoogervorst *et al.* has fewer openings than the cast in our study. The thickness of the cast is not given, this is a minor limitation. Our cast is 3.5 mm thick. The looks of the designs are similar, although the design of Hoogervorst *et al.* is more fluent. In our study, a maximum of 7.6, 8.1, and 5.5 degrees of displacement were present for extension, flexion, and ulnar deviation. Meaning the cast did not immobilize the fracture perfectly. However, this range of displacement is small, it is not known what this kind of influence on the movement/rotation has on the healing process. It is hard to describe whether the study of Hoogervorst *et al.*, can be compared to our study, as the test setups, loads, design and materials of the casts were all different. The result of our study does not show whether mechanical properties are sufficient for a DRF to heal. Furthermore, it is

not known what kind of maximum displacement is allowed for healing. Naturally no displacement would be the best.

The first limitation of this study was that two printed 3D casts did not fit well and were therefore excluded. The two casts left unsupported room between the cast and the wrist, and this was more than 1.0 cm around the wrist. It was not perfectly clear why the two casts did not fit well. This may have been caused by the process of frosting and defrosting the arm and therefore affecting the shape and size, which could affect the 3D scan and, therefore, the cast. Perhaps the first arms were in a slightly frosted state and, during the experiment, completely defrosted and would, therefore, not fit perfectly. As two casts were excluded, eight casts remained for the cantilever test. A larger group would provide more power and, therefore, more convincing conclusions.

Another limitation is the software used for the design of the surgical cutting guides. The program (Meshmixer) is not easy in use and does not allow for exact editing. Meaning that for example, a cutting line was edited to twenty degrees based on the function in Meshmixer. Each model has its own center, and the function is based on these centers. Therefore, it was not possible to exactly make all the surgical cutting guides the same way. For that reason, the guides are a little bit different. This led to different fracture angles. Additionally, the slit of the guide was set to 2 mm, where the osteotome was 1.2 mm. This means there was space between the slit and the osteotome. This could have led that the osteotome was not placed perpendicular, which could have altered the fracture angle. Although the surgical cutting guides were not perfect, the simulated fractures are all classified as Colles fractures [10].

Two surgical guides cracked during the fracture simulation phase. The osteotome was smaller than the slit in the guide. However, to simulate the fracture, the osteotome had to be placed in the whole width of the slit, and this led to the angulation of the osteotome. The osteotome is not exactly placed perpendicular to the radius. This probably resulted in contact between the osteotome and the guide. Now when the hammer hits the osteotome the forces are also translated to the guide. In this case, the material could not withstand the angular momentum of the osteotome and hammer. So in these cases, the fractures were simulated free hand after a begin of the fracture was simulated. Although a begin of the fracture was made, this could alter the intended fracture angle. However, the fractures were simulated straight and looked the same as the other fractures.

During the cantilever, test was experienced that an extra fixation pin was needed to fixate the arms to the base plate. This pin was hammered through the base into the forearm.

The loads chosen, were day-to-day loads, weights that are equal to, e.g., two bottles of water or a flask of laundry detergent. The chosen weights are not representative of the maximum load, as four kilograms does not come close to the maximum load in daily life. However, the loads provide a good indication of the loads in daily life, as e.g., picking up a glass or a bottle weighs not more than two kilograms. The cast should withstand forces/isometrics moments that can be generated by patients with DRFs, if this is achieved is not known. And should be investigated in future research.

Conclusion

This study showed that displacement is caused when a load is placed on an immobilized human cadaver model with a simulated DRF. The cantilever test showed to be efficient and sturdy in testing the human cadaver models. The simulated fractures were all Colles fractures, although the fracture angles were different because of the workflow in the design of surgical cutting guides. It remains unknown whether the cast provides sufficient immobilization properties.

Therefore, future research should focus on the immobilisation properties of the cast. Additionally, future research should focus on the improvement of the design, material selection, and processing.

Pilot Study

Introduction

Minimally angulated Greenstick and torus/buckle fractures are fractures in which the cortex and periosteum of a bone bend and break on the outside while remaining intact on the inside [78]. The fractures are diagnosed by clinical findings and confirmed by X-rays [79]. Torus/buckle fractures are instigated by axial loading forces. This fracture is characterized by a bump without fracture lines radiographically [78]. Greenstick fractures are caused by bending forces and are characterized by a radiographical gap at the apex of the fracture while on the opposite side the bone remains intact [78], [80]. The name greenstick is an analogy to young trees, which tend to break on the outside instead of the shattering that occurs in older and hardened trees. Naturally, these fractures occur most often in children between 4-15 years old [36], [81]. These fractures are usually caused by rotational trauma, of which the most common cause is a fall on an outstretched hand [78]. The fractures are represented in Figure 14.

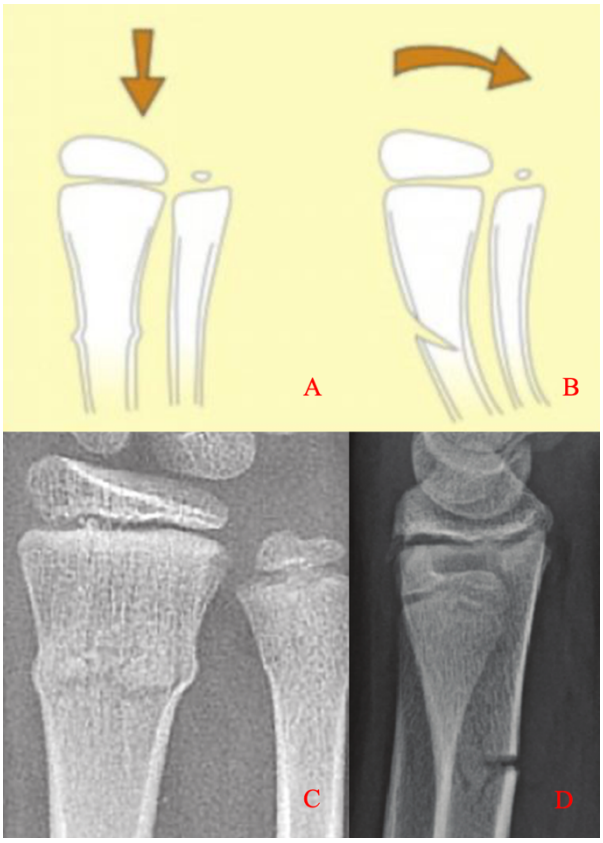

Figure 14: A), Buckle/torus fracture pattern as a cause of loading force (red arrow), B) Greenstick fracture caused by a bending force (red arrow) where the Ulna remains intact, C) a radiographic image of a buckle/torus fracture, D) a radiographic image of a greenstick fracture [82]–[84].

These fractures are treated either with immobilization for a short period of time with plaster or a pressure band and a sling. Greenstick and torus/buckle fractures are mostly stable and heal without complications with both treatment options. [85] Plint *et al.* showed that immobilization of the greenstick and buckle fractures through either plaster casting or bandage therapy is equally efficient in fracture stabilisation and pain relief [85]. However, both treatments have several disadvantages, including hygiene, skin complications, and weight in case of plaster [21], [26].

Another treatment option could be 3D-printed splints, braces, or orthosis, which hypothetically could exhibit fewer complications and equal treatment quality through a patient-tailored fit. One challenge of 3D-printed casts is the feasibility of their clinical practice. This study, therefore, aims to assess three aspects of 3D casts treatment, including the feasibility of the implementation of DRF with 3D-printed casts, the clinical outcomes (wrist function test documented in electronic patient dossier (EPD)), as well as patient experiences (complications, comfortability, restrictions of daily activities, patient satisfaction, and quality of life).

Methods

Inclusion

A nonscientific medical research (non-WMO) statement was obtained from the medical ethics review committee (METC), see Appendix 1 for the research protocol. Patients of 4 to 15 years that presented themselves between the 25th of July 2022 and 9th of September 2022 at the ER of the ETZ with a greenstick or buckle/torus fracture were eligible for inclusion. Patients that were not able to communicate properly (address pain or discomfort) and patients with comorbidities were excluded. Children and (foster)parents that did not master the Dutch language were also excluded.

Printing

The wrist casts were printed with Formlabs 3 (Formlabs Inc., Somerville, MA, USA). The color resin was used as materials. The print settings were full raft, layerthickness of 0.2 mm. The cast will have a Voronoi pattern design which is proven to provide adequate stabilization and immobilization properties and is comfortable and easy to use for both the patients and the clinicians [60], [61]. One challenge of 3D-printed casts is the feasibility of their clinical practice.

Workflow

A patient comes to the ER with suspicion of a DRF. First, an X-ray is made. When a greenstick or buckle/torus fracture is diagnosed, the patients and (foster)parents are inquired about the study. Informed consent was asked after a comprehensive explanation (see Appendix 2 and 3 for information letter patient and (foster)parent(s)) of the study design and aim. In case informed consent was not obtained, the patient received traditional treatment. If consent was provided, the forearm of the patient was scanned (with EinScan H) to obtain a 3D model. To scan the patient, the patient was seated on a bed, with the forearm in front of them and with the elbow supported on the thigh or knee of the patient with the hand in a relaxed position and the thumb in abduction. In case of motion and possible artifacts, the (foster)parent(s) were asked to hold the fingers of the patient for better stabilization (see Figure 15A). To cover the time needed to produce (see Figure 15B, C) the 3D-printed cast, the patients received temporary pressure bandages. After 24-48 hours, the patient returns to the hospital to check the fit of the 3D-printed cast.

Within 48 hours, the patients returned to the hospital. The pressure bandage was removed and changed for the 3D-printed cast. The researcher inspected if the cast had a perfect fit (no room to move, no pressure points that caused pain or irritation (if present the cast was sanded with 120 and 240 grit sandpaper) (see Figure 15D,E)). If the fit was not perfect, the patient received traditional plaster casting. When the cast fits, the patient receives instructions (see Appendix 2,3) and questionnaires. The patients were discharged and received an invitation for a two-week follow-up.

During the period of two-three weeks, the patients were allowed to move. However, the patients were instructed to stop if pain was present.

An evaluation of the wrist function was carried out after these two weeks. Range of motion was tested by executing the following movements: flexion, extension, radial deviation, ulnar deviation, pronation, and supination. The outcomes were documented in the Electronic Patient Dossier (EPD).

Additionally, the patient and (foster)parent(s) were asked to fill out a questionnaire on the experience of the new treatment. In case of adequate recovery, the patient was discharged. In case of pain or reduced wrist function, the treatment was continued for another week as this was deemed a sufficient time for regaining function.

During the period of the treatment, the patient and (foster)parent(s) were instructed to contact the hospital if any complications were present. Treatment consequences were evaluated by a clinical technician and surgeon, and the best strategy was reported back and discussed with the patient and his or her parents.

Questionnaire

The children's questionnaire was a Visual Analogue Scale (VAS) score based on smileys, ranging from 1 (never/great) to 5 (often/bad). The children's questionnaire is presented in Appendix 4, and the parent's questionnaire is presented in Appendix 5. Both questionnaires were in Dutch.

Apart from the questionnaires, the total time of the design and production workflow was measured, and the number of hospital visits was registered.

Results

A total of four individuals aged 4-6 years presented themselves at the hospital with a greenstick or buckle/torus fracture between June and September 2022. Out of these four participants, a total of three patients provided informed consent for the study. One patient did not want to participate in the study due to logistic reasons. The mode age was 5 years old, all participants were female. More detailed baseline characteristics are provided in Table 10, together with the questionnaire scores of both the child and the (foster)parent(s). All patients regained wrist function after 2-3 weeks, the ROM was normal, no pain was presented after recovery.

As can be seen from Tables 10 and 11, both the children and parents were positive about the new treatment, scoring the treatment with an average of 9.0 out of 10.0 and preferring this treatment over traditional plaster casting in case of future fracture management. In the questionnaire of the patients, all parameters, except itching, were scored at least a two. The parameter itching scored an average of 3, meaning that every now and then, the patient suffered from itching. The average design-, printing-, and post-process time was 12 hours and 58 minutes.

The number of hospital visits was similar for all the patients, as they all visited the hospital three times. The first time was for the X-ray and the 3d scan of the forearm, the second visit was to fit the cast, and the third time was for an evaluation visit.

Patient two showed swelling larger than the offset of 0.5 mm during the second hospital visitation. After consulting the medical doctors, the patient was sent home with the 3D-printed cast as it was expected that the swelling was decreased enough after three days so that the 3D-printed cast would fit.

In the questionnaire of the (foster)parent(s), all parameters scored high, although the (foster)parents of the second patient scored the itching and pain in the middle. The questionnaires provided more insights. The (foster)patient(s) said that the casts were ideal because it gave their kids the freedom to swim on holiday. The patients were more independent, which is positive. However, the patient must not forget that the wrist needs rest to heal. This was emphasized during the first consultation and again during the second consultation. The (foster)parent(s) listed the following advantages: the cast was lightweight, caused less itching than plaster casting, gave no smells and no sweating, and was easy to clean. Moreover, the water resistance and improved hygiene were praised, causing the patient to be more independent. However, the (foster)parent(s) listed also points to improve: The Velcro arcs of the cast needed to be stronger, the variety of available colors could be larger, and the Velcro straps should be smaller in width. Further, the production time was listed as a disadvantage.

After two weeks, the patients came back for evaluation. For all the patients, the two weeks were adequate for healing. They regained full function and range of motion of the wrist.

During the pilot study, two minor changes were made to the design. The first change was the design of the arcs. The arcs were made tougher and thicker to prevent the arcs from breaking. The second change was that the Velcro straps were halved in width to prevent skin irritation due to friction.

Table 10: Outcomes of the questionnaire of the patient

	Score		
Question/Patient characteristics	Patient 1	Patient 2	Patient 3
Age	4	5	6
Gender	Female	Female	Female
Fracture type	Greenstick	Greenstick	Greenstick
Laterality fracture	Left	Left	Right
Dominant hand	Right	Left	Right
Number of hospital visits	3	3	3
Design and production time* (in hours and minutes)	*12:43*	*12:55*	*13:13*
Itching	4	3	2
Sweating	2	1	1
Smell	1	1	1
Pain	1	1	1
Skin irritation	1	1	1
Weight	1	1	1
Bathing	1	1	1
Look	2	1	2
Daily activities	2	2	2
Preferred future treatment	3D cast	3D cast	3D cast

*is the time for printing the 3D cast and the postprocessing time

Table 11: Outcomes of the questionnaire of the (foster)parent(s)

	Score		
Question/Patient characteristics	(foster)parent(s) 1	(foster)parent(s) 2	(foster)parent(s) 3
Daily activities	1	3	2
Skin irritation	1	0	0
Itching	2	5	0
Weight	0	0	0
Smell	0	0	0
Pain	0	5	0
Bathing	1	0	0
Sleeping	0	0	0
Treatment score	9	8	10
Look	9	8	9
Preferred future treatment	3D cast	3D cast	3D cast

Figure 15: Images of the products of the workflow. A) 3D scan of the arm, B) first step of the design, C) the final design, D) picture of the dorsal side of the 3D cast worn by the patient, E) the anterior side of the 3D cast worn by the patient.

Discussion

The aim was to investigate the feasibility of 3D-printed casts in the clinic for the treatment of distal radius fractures. Therefore, different aspects were analysed: feasibility of the implementation of DRF with 3D-printed casts, the clinical outcomes, and patient experiences (complications, comfortability, restrictions of daily activities, patient satisfaction, and quality of life). Although there were just three patients, the workflow proved to be feasible (Table 10) and practical to implement 3D-printed casts in the clinic. Every patient received their cast within 24 hours (the average time was 12 hours and 58 minutes). Additionally, the pilot study showed that the clinical outcomes were positive; every patient recovered from their DRF. The patients and the (foster)parent(s) listed a lot of advantages (the cast was light, caused less itching than plaster casting, gave no smells and no sweating, and was easy to clean). Major advantages were the water resistance and improved hygiene, giving the patient more freedom and, therefore, also giving the (foster)parent(s) more freedom. Our results are in agreement with other literature, like Keller *et al.* and, Lazzeri *et al.*. They reported similar outcomes in comfortability and the feasibility of printing 3D cast in the clinic.[45], [57] Further, Chen *et al*., and Lazzeri *et al.*, showed the same sort of clinical outcomes, as the patient's recovered fully [24], [57]

Based on the consults and the questionnaires, the patients were enthusiastic. The conclusion of the questionnaires was that the cast caused no pain, gave no smell, easy to bath with. The patients suffered from mild sweating. No pressure points were present. This was achieved as all the cast were sanded after printing. The patients were happy with the looks of the cast. However, the patients did suffer from itching. Whether the itching is less or more present than during plaster treatment remains to be elucidated. During the control consult, the patients and the (foster)parent(s) pointed out that the cast allowed more participation in the activity of daily living and would therefore choose the 3D-printed cast over plaster. The (foster)parent(s) did not list the extra visit as a disadvantage.

The major limitation of the current study is the lack of a control group, which made it impossible to statistically compare 3D cast therapy with current gold standards. Another limitation of the pilot study is the limited number of included patients, which diminishes external validity. The results of the current study should therefore be interpreted as exploratory rather than hypothesis-proving.

A limitation is the printing time. The total time of the workflow was within 24 hours. The average printing time was about twelve hours, so up to 50%, time was printing time. The difference in printing time is caused by the different sizes of the patient's forearms. One solution to this problem is to use newer and quicker printers. Such as digital light processing (DLP), Xkelet (a company that provides 3D-printed orthosis) demonstrated that a time frame of 3-4 hours to print orthosis for adults is feasible (and maybe even faster). However, DLP printers are more expensive than SLS printers. The cost of materials ranged from €12,50 to €15,90. These material costs are higher than the cost of plaster (which costs only a few euros [86]).

The swelling of the arm in the first few days after the DRF was a limiting factor for 3D printing implantation as well, as it impairs patient-tailored 3D construction through intra-individual variability of arm size over time. In the current design, the offset was 0.5mm, allowing for a 1 mm swelling around the wrist in every axis. In the case of patient two, this offset was not enough for the first few days. This resulted in removing the pressure bandages after three days. After three days, the cast fits due to swelling loss. There is no literature is found on a numeric average of the swelling in the case of a DRF. To improve the fit of 3D-printed patient-tailored casts in the future, further research is necessary for a better understanding of the maximal swelling and the decay of the swelling during a greenstick fracture of the arm. A predictive model of the swelling can help to improve the fit of the 3D-printed cast after scanning the arm in the first days. However, even if the prediction is more precise, a cast fitting both

the excessive swelling and the decayed swelling is challenging to design. To account for this problem, there must be a possibility to tighten or loosen the cast without changing the stabilization properties of the cast. In the design of the cast this is achieved with the Velcro wraps, which allow to adjust (tying the wraps tighter or looser) for the tightness.

After the first patient, a small change was made to the arcs. The arcs which guided the Velcro straps were, in the first instance, too thin and cracked. Although it has no consequences if the arcs breaks, the design was adjusted with thicker arcs, to prevent breakage. Another small change was that the Velcro straps were halved in width at the distal end of the cast, as the strap caused skin irritation due to friction.

The last point of improvement based on the questionnaires was that the choice of color could be larger than orange and blue. Another possible improvement could be smoothing the design in Meshmixer make the post-processing less intensive and making the cast more comfortable. This could be achieved with Meshmixer and the functions reduce and smoothing. A possible outcome is displayed in Figure 16.

A randomized controlled trial (RCT) should be conducted to show if the treatment with 3D-printed cast is better than plaster casts. The new treatment scored an average of 9.0 out of 10.0, and is preferred over treatment with traditional plaster casting. A lower score is expected for the plaster casts as in 30% of the cases are complications. However, this needs to be proved.

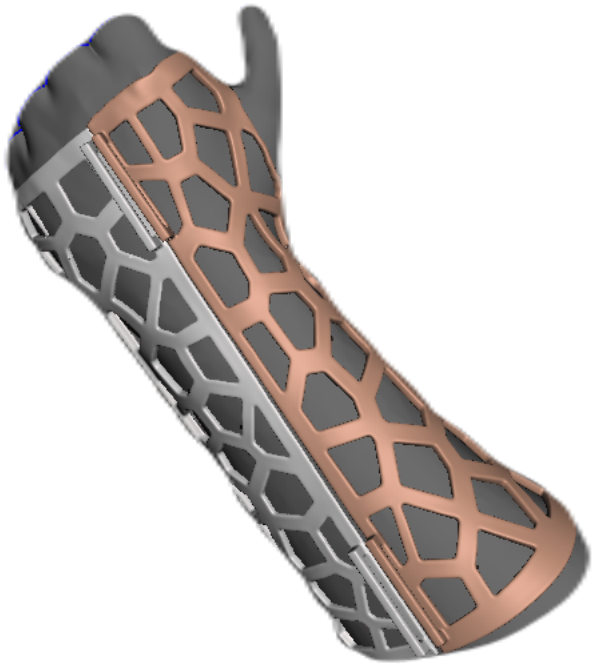

Figure 16: Possible improvement of the 3D-printed cast

Conclusion

The pilot study showed that it is feasible to implement 3D-printed casts for the treatment of greenstick fractures of the forearm in a clinical setting. In this study, a cast was produced and fitted within 24 hours after presentation at the ER. The patients recovered functionally, and pain and swelling were completely gone after two weeks. Both the patients and the (foster)parent(s) were scored the treatment with a 9.0 out of 10.0, stating a preference for a 3D cast over traditional plaster. A randomized control trial comparing 3D-printed casts with plaster casts will be essential to providing evidence for its use in clinical practice. Future improvements will need to focus on shortening printing duration and providing an adjustable fit to account for variable and time-dependent swelling of the arm after a greenstick fracture.

Orthosis for wrist arthrosis

Introduction: patient case

A patient with severe rheumatoid arthritis in both hands, and mainly the thumbs (female, 63 years old), has negative experiences with her brace. It did not provide enough immobilization and support for the metacarpophalangeal joint (MCP) and the carpometacarpal joint (CMC) (see Figure 17 for the traditionally made brace/orthosis). Furthermore, the process of making the brace is not comfortable. During this process, the material is heated up to a temperature of 65-70 degrees and placed on the skin. The brace stimulates perspiring (mainly in summer), which causes poor hygiene and bad smells. Further, the brace is easily damaged due to ADL. Additionally, the brace did not support the patient in her ADL. Performing tasks in daily life was not effortless or smooth.

The production of an orthosis like this can be improved by a 3D scanner. A scan could be made in one or two minutes, has no radiation, and provides no pain for the patient. Furthermore, the material used for the traditionally made brace, Orfilight Black NS is less wear-resistant, tough, and breaks sooner compared with color resin (material of Formlabs, Orfilight versus Resins: Tensile strength 8 MPa – 65 MPa, Tensile modulus 160 MPa – 2.8 GPa, Flexural modulus 260 MPa – 2.2 GPa).

As the previously conducted pilot study showed, it is feasible to print a cast within an acceptable time frame. A case study is conducted to investigate the applicability of 3D printing in orthopedics with another purpose than the immobilization of a fracture. Therefore, we asked the patient if she wanted to contribute to a case study when we tried to create a thumb orthosis to overcome these issues.

Figure 17: the traditionally made brace

Method

Orthosis

3D scan

After an explanation of the case study and showing the first possible design of the brace, the patient was asked to participate. The patient wanted to participate, and informed consent was signed. The orthosis was worn for one week during the activities of daily living. After this week, feedback was provided. Based on the feedback, it is determined whether the 3D-printed brace was supporting here more in ADL.

A 3D scan was made of both hands separately in a relaxed/neutral position (Figure 18). The model was loaded into Meshmixer (AutoDesk, Inc., San Rafael, USA). The data can be altered with Meshmixer to immobilize the MCP and CMC joints better than the traditional brace. To create an orthosis, the following steps must be taken in Meshmixer:

- In Meshmixer, the fingers and forearm are removed from the data, using the Plane Cut function with the No Fill option.
- To prevent excessive tightness of the cast, a small offset of 0.5 mm in the normal direction was put in place by selecting the trimmed surface and using the Offset function.
- The model is processed so that the dorsal side of the hand is removed, and the hand fits the orthosis without changing the hand posture.

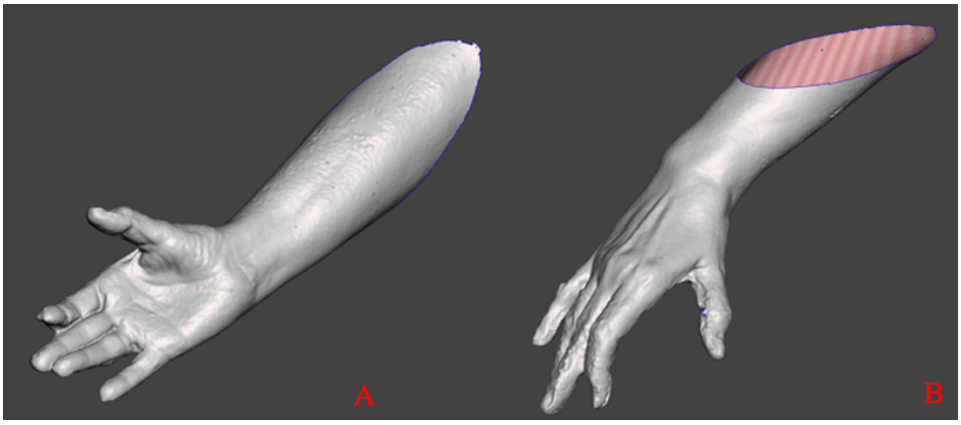

Figure 18: scan of the patient's hand. A) the frontal side of the 3D scan, B) the dorsal side of the 3D scan.

Creating the orthosis

A semi-automated algorithm in Rhino 6 was used to design the orthosis, with the addition of RhinoResurf (Trunhoo Network Technology, Nanjing, Jiangsu, China), Grasshopper, and Grasshopper LunchBox plugins. The methodology is like the method used for designing the wrist orthosis. One difference is that the number of Voronoi cells will be less than the casts created earlier, while the orthosis is smaller than the wrist cast. An arbitrary number was chosen for the Voronoi cells. In both braces, the number was 15.

The thickness of the orthosis was set to 5 mm which, will allow for support without burden on the MCP and CMC joints. An arc was added to allow closure with a Velcro strap. The orthosis surface was then smoothened (smoothing setting: Shape persevering, smoothing factor = 1, smoothing scale = 4, constraint rings = 3), which can help to provide a more comfortable feeling of the orthosis.

The orthosis was then printed with color resins. The print took almost 10 hours to print and used 60 ml of resin, which cost around €10 (including VAT). All these steps are displayed in Figure 19. The orthosis was sanded (120 and 240 grit sandpaper) to further smoothen the surface of the orthosis.

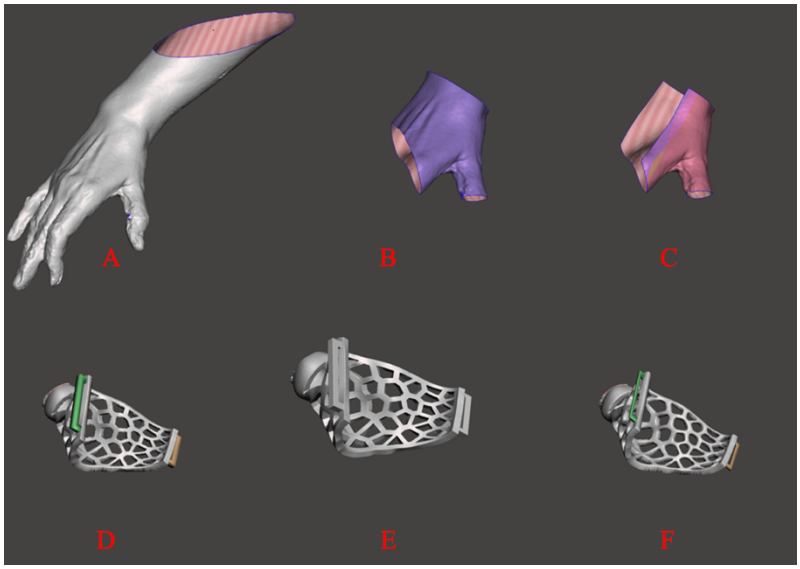

Figure 19: workflow and finished product. A) the 3D scan of the arm, B) The arm and fingers are removed, C) an open brace is made to allow the hand to go in the brace, D) the semi-automated algorithm makes the pattern, thickness and in Meshmixer, the arcs are added, E) the model is made solid, F) the design is smoothed.

Results

The brace allowed the patient to carry a bag with her hand, which was first not possible. In Figure 20, the patient wears the orthosis, which shows that the fit was perfect. The fit of the orthosis was excellent, and it was established that the brace provided more support in the activity of daily living based on her feedback. The brace was more comfortable than the traditionally made brace. The most important difference is that the thumb is more fixated without any pain or irritation. In Figure 16, there is room around the thumb to move. Figure 19 shows that there is no space between the thumb and the brace, as it is enclosed. The perceived effort of daily activities and pain was lower during these activities with the orthosis compared to the traditional brace. While working, the orthosis supported her activities, and she worked longer without pain. Another observation was that the brace supported her more than the traditional brace, as she stood up easier out of her chair. One more advantage was the decreased sweat production and the possibility of cleaning the orthosis.

Due to varying degrees of inflammation, pain, and swelling that are changing day by day, the patient did not wear the brace all day long. However, this brace provided more support and functional immobilization of the joints than the traditionally made brace.

Figure 20: the orthosis on the patient's hand.

Discussion

The aim of this patient case was to investigate the applicability of 3D printing in orthopedics with another purpose than immobilization of a fracture. The patient's case showed that the workflow is practical and feasible to print a brace this size within 24 hours, and the 3D printing can have an additive value not only for fractures but also for patients with rheumatoid arthritis.

The patient performed activities of daily living with less effort and the patient suffered from less pain while performing these tasks. The patient was satisfied with the brace, as the patient could participate more in ADL. Normally for these activities, the brace was taken off. As the brace gets wet. It was mentioned that often after the brace was taken off, forgotten to put the brace back on as it was not comfortable. This was not the case with the new brace, the brace was not taken off for ADL, and it can get wet and is more comfortable. We hypothesize that the orthosis printed in the current study provides better support through a higher rigidity than the conventional treatment. As 3D-printed brace enclosed the thumb perfectly, it provided better support. The material used showed to be more rigid. The 3D-printed brace gave an optimal balance between rigidity and suppleness, as she could stay active while her thumbs were supported.

One of the major advantages was that the brace could withstand pressure. E. g. the patient used her hands to stand out of a chair with no or less pain in her hands. The orthosis was used either as a joint stabilizer, a tool for heavy tasks, or a preventer of the deteriorating effects of osteoarthritis on the MCP and CMC joints. The brace/orthosis had a better fit than the traditionally made orthosis.

The orthosis/brace was 5 mm thick. This was thicker than the 1.6 mm of the traditional brace. However, the weight of both braces (27 grams for the traditional brace and 37 grams for this brace) were comparable. Ten grams of difference did not hinder the patient in ADL. The brace has characteristics that are comparable to the brace from Mohammed *et al.* [87]. In this study, the aim was to demonstrate that it is feasible to design and produce low cost, rapid design of a brace. However, no costs of the product are known. Our brace costs around €10 (including VAT).

The production process was a positive point. A 3D scan is made within one minute, and the thumb orthosis is created within 24 hours. Although the production time is longer, the patient does not have to suffer to produce the brace. As for the traditional orthosis, her hand needed to be wrapped with hot material, which was a painful procedure.

A disadvantage of the cast was that the first time wearing the orthosis, the patient suffered irritations on the skin due to pressure points. This was caused by the support material, which is removed after washing and curing. As the support is removed, it can leave spots sometimes, this could give pressure points. In this case, it was quickly resolved by sanding the orthosis; after this, no pressure points were present.

An important limitation of the current study is its sample size. A randomized control trial should be conducted to assess whether a 3D-printed brace is better than the traditional brace.

In the literature, there is no clear consensus about what the ideal orthoses should be [88]. Therefore, a biomechanical study should be performed to gain knowledge about what the ideal brace is, whether e.g. the pressure on the fingers is measured to establish what pressure is needed for immobilization and what pressure leads to complications.

Conclusion

The ability to create individual, open-latticed braces could leads to new opportunities for the implementation of 3D technologies into the orthotics workflow. Patients could be helped better by 3D technologies in the field of orthotics for chronic pain and for long-term upper extremity treatments. 3D printing can be a solution for designing personalized orthosis for patients with arthrosis.

General discussion and conclusion

Key findings of this thesis include the proof of concept of the working mechanism of the orthosis in the cadaver study and the demonstration of the feasibility of small-scale implementation of a workflow for 3D printing orthosis. In addition, this thesis shows the perceived improvement of participation in activities of daily living with a 3D-printed orthosis compared to standard care, and the decrease of perceived pain, itching and sweating in patients with a 3D-printed orthosis.

Strengths and limitations

This thesis contains a multilayered study that researched which material is the best for FDM printing. Furthermore, it showed that it is feasible to use a 3D-printed cast for DRFs. The pilot study demonstrated it is feasible to print casts within an acceptable time (24-48 hours) for the patients. Furthermore, both the patients and the patient's parents, as well as the medical staff, were enthusiastic about the 3D-printed casts. The theoretical benefit showed to be practical benefits in real life as well. The cadaver study showed that there is displacement after load in human cadaver models.

Furthermore, the exploration of other areas, such as a brace for therapeutic means with patients with arthritis, showed a new extra manner to support the patients.

There are a few general limitations. Starting with the printing time, it took around the 24-48 hours to print a brace or a cast, depending on the size of the patient's extremity. In the future, this should be less than a few hours. A bridging treatment is currently necessary before the casts are printed. Quicker printing techniques are available and are developed every year (e.g. digital light processing printers (DLP), or to choose for an industrial printer with larger capacities). Furthermore, it becomes cheaper every year. Another limitation is the build volume. The cast for the pilot study was printed in the Form 2 and a Form 3 SLA printer from Formlabs. The size of the possible prints was limited by the build volumes, which are 14.5 × 14.5 × 17.5 cm and 14.5 × 14.5 × 18.5 cm, respectively. This build volume does not allow for printing cast for adults, and therefore we opted to use the Ultimaker printer for the cadaver study. The printing quality of the orthosis of the cadaver and the pilot study differ and are not directly comparable.

Another limitation is the cost-effectiveness. The acquisition of 3D printers, materials, a 3D scanner, and qualified staff, is expensive. Furthermore, the manual labor of the design and post-processing of the casts takes time. Faster and cheaper printing techniques might negate these disadvantages partially in the future. The manual labor could be made less intensive by using applications like Spentys or Xkelet. These paid applications scan the extremities and automatically design a ready-to-print cast.

Future perspectives

During this graduation internship, the focus was on 3D-printed wrist casts for DRFs. It has proven to be a promising solution for the treatment of DRFs. In this study, stable fractures were studied. Unstable fractures were not the focus of this study. However, a 3D-printed cast may also be a promising solution for unstable DRFs.

Orthopediatrics

The pilot study showed that 3D-printed casts are feasible to implement in the clinic. It seems interesting to investigate if 3D-printed orthosis or braces can be used for other treatments. Examples where 3D-

printed, could be a solution is an elbow cast, an ankle cast, a foot cast, a sleeve to prevent foot drop, sole to prevent/treatment of diabetic foot ulcers (offloading techniques). These can be achieved with a few or no alterations of the same design algorithm. The extrapolation of the use of 3D-printed casting to other treatments or therapies seems a logical follow-up step. By exploring other functionalities of 3D printing, 3D printing becomes more efficient and readable.

The patient case study showed another possible application of 3D-printed orthosis. 3D printing for patient-specific solutions, and especially for devices that are intended to use for a longer period, could play a big role in orthopedics and other departments. For example, arthritis is one of the most common conditions where joint disorders are present. Treatment consists of pain relief, physical therapy, standard braces, and even surgical treatment (Arthroplasty is a last resort, while this is expensive and is not lasting a lifetime) [88]. 3D-printed braces may help better, as traditional braces often fall short of optimal fit and patient expectations, resulting in less than optimal immobilization of joints and lack of use of the brace. [87]. However, the area is still evolving. Therefore, future research should focus on functionality, materials, comfort, and design requirements to relieve the pain of the patients and improve the Quality of Life (QoL) of patients.

In literature, 3D printing technology is already used to investigate the applicability for treating scoliosis [89], 3D printed soles for patients with symptomatic flatfoot, plantar fasciitis [90]–[92]or diabetic feet, specific ankle-foot orthoses for persons after stroke [93] and, 3D-printed orthosis for patients with peripheral nerve injuries [47].

For the design of the casts, the limitations were the thickness and the ratio of stiffness and ventilation. The thickness was based on the thickness of the plaster cast. However, it remains unclear whether this is the ideal thickness of the 3D-printed casts. As this was not the topic of this research. The thickness was the same as a plaster cast, and perhaps this thickness could be less to improve comfort. The ratio of stiffness and ventilation holes was chosen based partially on the printing time. Future research should focus on improving the design as it's not known what kind of biomechanical properties (thickness, ratio of stiffness and openings) are needed to immobilize a fracture. Although 3D printing is promising, most published literature using 3D-printed casts are still in the concept stage or initial phase [19], [94]. Therefore, more research with experimental data and clinical experiences are necessary. One manner to gain more knowledge is to perform a finite element (FE) analysis. FE can help surgeons to better understand the biomechanical features of injured tissues and involve medical devices [58], [95]. FE simulation predicts changes in stress distribution and fracture displacement. The biomechanical properties of a casted forearm with a DRF is not clear. In Chen *et al.,* an integrated finite element (FE) model was conducted to gain more knowledge about the biomechanical features of the fractured bone of the forearm with a 3D-printed cast [58], [95]. In this model, the radius and ulna were cut through to mimic the bone fracture. Then a force and rotational moment are applied to the cast (not directly to the hand). The results showed that the cast was able to maintain shape and function without a displacement of the fracture. In our cadaver's study, forces were applied directly on the hand to study the effect on the simulated fracture. Chen's study could be repeated with our design to investigate the immobilizing properties. A step further can be to analyze different kinds of designs with different thicknesses, ratios of stiffness and ventilation, can be analyzed.

Printers

In this thesis, two kinds of printers are used, FDM and SLS printing. Both types of printing have their advantages and disadvantages. With the cadaver study, the Ultimaker S5 was used, which uses the FDM technique. Here was shown that the surface finish was not great, as the layers could be distinguished without difficulty. One possibility to improve this is sanding. Although this could be an intensive process, further exploration of FDM printing and post-processing could be promising as the printers become more accurate, faster, and cheaper. Further, it is interesting as the material costs are low, and FDM-suitable materials have less impact on the environment. As the materials have the possibility to be recycled or the materials are biodegradable. For the pilot study, the Formlabs 3 was used, which uses the SLS technique. Here the cost was a limiting factor. For both printers, time was a big disadvantage. Printing took 12-36 hours to print one orthosis (for the casts of the cadaver study). Xkelet, a commercial company, uses DLP. This company can print braces within 3-4 hours, dependent on the size. This is a major advantage. Hopefully, in the future, printers will become faster and cheaper and have a selection of materials that will be recyclable.

Materials

In our study, a few of the many available materials were selected. In our selection, a few criteria were used, and one important criterion for the future was recyclability. Hopefully, soon, there will be recyclable thermosets that are suitable for SLS printers. If this is the case, then the use of these printers will be preferable over FDM. This is because the surface finish is superior, as each layer is fused with the previously printed layer.

Conclusion

The aim of this thesis was to investigate whether 3D casts can replace plaster casts with non-displaced Colles fractures. In this thesis, it is shown that PLA is most suitable and compared to plaster based on literature and printing expertise. The pilot study has shown that it is possible to implement a workflow that allows printing the cast within 24-48 hours. Furthermore, in the pilot- and case study, the patients, (foster)parent(s), and the medical staff had positive experiences with 3D-printed casts and braces. Furthermore, the human cadaver study showed the immobilizing abilities of the cast. However, a direct comparison with plaster could not be made. An RCT will be necessary to investigate if the use of 3D-printed casts is superior to plaster casts in joint immobilization and quality of life. In addition, more research should be conducted to make the manual labor less intensive using automatic applications (Xkelet, Spentys), the exploration of treatment with 3D-printed casts for unstable fractures and treatments with 3D-printed casts for other extremities, and the field of orthopedics.

Literature

[1] Ç. Ayhan and E. Ayhan, "Comparative Kinesiology of the Human Body: Normal and Pathological Conditions," pp. 211–282, 2020, [Online]. Available: http://www.sciencedirect.com/science/article/pii/B9780128121627000138

[2] R. A. Berger, "The anatomy and basic biomechanics of the wrist joint," *J Hand Ther*, vol. 9, no. 2, pp. 84–93, 1996, doi: 10.1016/S0894-1130(96)80066-4.

[3] J. A. N. Verhaar and J. B. A. van Mourik, "Het lichamelijk onderzoek," *Leerboek orthopedie*, pp. 3–21, 2019, doi: 10.1007/978-90-368-2276-3_1.

[4] C. Scheuer *et al.*, "Grabb and Smith's plastic surgery: Seventh edition," *Physical Education and Sport for Children and Youth with Special Needs Researches – Best Practices – Situation*, pp. 343–354, Sep. 2013, doi: 10.2/JQUERY.MIN.JS.

[5] J. R. Sheen and V. v Garla, *Fracture Healing Overview*. StatPearls Publishing, 2022. [Online]. Available: https://www.ncbi.nlm.nih.gov/books/NBK551678/

[6] Adler C. P., *Pathologic bone fractures: definition and classification. Langenbecks Archiv fur Chirurgie. Supplement II, Verhandlungen der Deutschen Gesellschaft fur Chirurgie. Deutsche Gesellschaft fur Chirurgie*. 1989.

[7] J. L. Marsh *et al.*, "Fracture and dislocation classification compendium - 2007: Orthopaedic Trauma Association classification, database and outcomes committee," *J Orthop Trauma*, vol. 21, no. 10 Suppl, 2007, doi: 10.1097/00005131-200711101-00001.

[8] P. Jayakumar, T. Teunis, B. B. Giménez, F. Verstreken, L. di Mascio, and J. B. Jupiter, "AO Distal Radius Fracture Classification: Global Perspective on Observer Agreement," *J Wrist Surg*, vol. 6, no. 1, p. 46, Jan. 2017, doi: 10.1055/S-0036-1587316.

[9] M. E. Müller, P. Koch, S. Nazarian, and J. Schatzker, "The Comprehensive Classification of Fractures of Long Bones," *The Comprehensive Classification of Fractures of Long Bones*, pp. 106–115, 1990, doi: 10.1007/978-3-642-61261-9.

[10] E. G. Meinberg, J. Agel, C. S. Roberts, M. D. Karam, and J. F. Kellam, "Fracture and Dislocation Classification Compendium-2018," *J Orthop Trauma*, vol. 32, 2018, doi: 10.1097/BOT.0000000000001063.

[11] H. M. J. Janzing *et al.*, "Treatment of dorsally dislocated distal radius fractures with individualized 3D printed bracing: an exploratory study," *3D Print Med*, vol. 6, no. 22, pp. 1–7, 2020, doi: 10.1186/s41205-020-00075-4.

[12] M. M. J. Walenkamp, L. M. Vos, S. D. Strackee, J. C. Goslings, and N. W. L. Schep, "The Unstable Distal Radius Fracture—How Do We Define It? A Systematic Review," *J Wrist Surg*, vol. 4, no. 4, p. 316, Jan. 2015, doi: 10.1055/S-0035-1556860.

[13] K. W. Nellans, E. Kowalski, and K. C. Chung, "The Epidemiology of Distal Radius Fractures," *Hand Clin*, vol. 28, no. 2, p. 113, Jan. 2012, doi: 10.1016/J.HCL.2012.02.001.

[14] E. R. B. Stirling, N. A. Johnson, and J. J. Dias, "Epidemiology of distal radius fractures in a geographically defined adult population," *J Hand Surg Eur Vol*, vol. 43, no. 9, pp. 974–982, 2018, doi: 10.1177/1753193418786378.

[15] A. Bentohami and printing: I. P. design, "Fractures of the distal radius: Epidemiology, treatment and outcome," p. 114, 2021.

[16] J. B. Sintenie, J. H. Allema, and B. Ivanyi, "Fracturen bij kinderen." pp. 87–109, 2019.

[17] S. Meena, P. Sharma, A. K. Sambharia, and A. Dawar, "Fractures of Distal Radius: An Overview," *J Family Med Prim Care*, vol. 3, no. 4, p. 325, 2014, doi: 10.4103/2249-4863.148101.

[18] E. A. Oakley, K. S. Ooi, and P. L. J. Barnett, "A randomized controlled trial of 2 methods of immobilizing torus fractures of the distal forearm," *Pediatr Emerg Care*, vol. 24, no. 2, pp. 65–70, Jan. 2008, doi: 10.1097/PEC.0B013E318163DB13.

[19] J. Graham, M. Wang, K. Frizzell, C. Watkins, P. Beredjiklian, and M. Rivlin, "Conventional vs 3-Dimensional Printed Cast Wear Comfort," *Hand (N Y)*, vol. 15, no. 3, pp. 388–392, Jan. 2020, doi: 10.1177/1558944718795291.

[20] A. Fazekas, R. Dendievel, L. Salvo, and Y. Bréchet, "Effect of microstructural topology upon the stiffness and strength of 2D cellular structures," *Int J Mech Sci*, vol. 44, no. 10, pp. 2047–2066, Jan. 2002, doi: 10.1016/S0020-7403(02)00171-6.

[21] F. Blaya, P. S. Pedro, J. L. Silva, R. D'Amato, E. S. Heras, and J. A. Juanes, "Design of an Orthopedic Product by Using Additive Manufacturing Technology: The Arm Splint," *J Med Syst*, vol. 42, no. 3, Jan. 2018, doi: 10.1007/S10916-018-0909-6.

[22] E. D. Shirley, K. J. Maguire, A. L. Mantica, and R. W. Kruse, “Alternatives to Traditional Cast Immobilization in Pediatric Patients,” *J Am Acad Orthop Surg*, vol. 28, no. 1, pp. 20–27, Jan. 2020, doi: 10.5435/JAAOS-D-18-00152.
[23] M. Halanski and K. J. Noonan, “Cast and splint immobilization: complications,” *J Am Acad Orthop Surg*, vol. 16, no. 1, pp. 30–40, 2008, doi: 10.5435/00124635-200801000-00005.
[24] Y.-J. Chen, H. Lin, X. Zhang, W. Huang, L. Shi, and D. Wang, “Application of 3D–printed and patient-specific cast for the treatment of distal radius fractures: initial experience,” *3D Print Med*, vol. 3, no. 1, Jan. 2017, doi: 10.1186/S41205-017-0019-Y.
[25] E. M. M. van Lieshout *et al.*, “Personalized 3D-printed forearm braces as an alternative for a traditional plaster cast or splint; A systematic review.,” *Injury*, vol. 53 Suppl 3, pp. S47–S52, Nov. 2022, doi: 10.1016/j.injury.2022.07.020.
[26] K. Boutis, A. Willan, P. Babyn, R. Goeree, and A. Howard, “Cast versus splint in children with minimally angulated fractures of the distal radius: a randomized controlled trial,” *CMAJ*, vol. 182, no. 14, pp. 1507–1512, Jan. 2010, doi: 10.1503/CMAJ.100119.
[27] M. S. Ghiasi, J. Chen, A. Vaziri, E. K. Rodriguez, and A. Nazarian, “Bone fracture healing in mechanobiological modeling: A review of principles and methods,” *Bone Rep*, vol. 6, pp. 87–100, Jan. 2017, doi: 10.1016/J.BONR.2017.03.002.
[28] P. Guida *et al.*, “An alternative to plaster cast treatment in a pediatric trauma center using the CAD/CAM technology to manufacture customized three-dimensional-printed orthoses in a totally hospital context: A feasibility study,” *Journal of Pediatric Orthopaedics Part B*, vol. 28, no. 3, pp. 248–255, Jan. 2019, doi: 10.1097/BPB.0000000000000589.
[29] M. Lafontaine, D. Hardy, and P. Delince, “Stability assessment of distal radius fractures,” *Injury*, vol. 20, no. 4, pp. 208–210, 1989, doi: 10.1016/0020-1383(89)90113-7.
[30] J. W. Andrushko, L. A. Gould, and J. P. Farthing, “Contralateral effects of unilateral training: sparing of muscle strength and size after immobilization1,” *Appl Physiol Nutr Metab*, vol. 43, no. 11, pp. 1131–1139, 2018, doi: 10.1139/APNM-2018-0073.
[31] A. C. Plint, J. J. Perry, R. Correll, I. Gaboury, and L. Lawton, “A randomized, controlled trial of removable splinting versus casting for wrist buckle fractures in children,” *Pediatrics*, vol. 117, no. 3, pp. 691–697, Jan. 2006, doi: 10.1542/PEDS.2005-0801.
[32] C. von Keyserlingk, K. Boutis, A. R. Willan, R. B. Hopkins, and R. Goeree, “Cost-effectiveness analysis of cast versus splint in children with acceptably angulated wrist fractures,” *Int J Technol Assess Health Care*, vol. 27, no. 2, pp. 101–107, Jan. 2011, doi: 10.1017/S0266462311000067.
[33] C. E. Hill, J. P. M. Masters, and D. C. Perry, “A systematic review of alternative splinting versus complete plaster casts for the management of childhood buckle fractures of the wrist,” *J Pediatr Orthop B*, vol. 25, no. 2, pp. 183–190, 2016, doi: 10.1097/BPB.0000000000000240.
[34] C. T. Price, “A splint was not inferior to a cast for distal radial fracture in children: Commentary,” *Journal of Bone and Joint Surgery - Series A*, vol. 93, no. 10, p. 970, Jan. 2011, doi: 10.2106/JBJS.9310EBO619.
[35] S. West, J. Andrews, A. Bebbington, O. Ennis, and P. Alderman, “Buckle fractures of the distal radius are safely treated in a soft bandage: A randomized prospective trial of bandage versus plaster cast,” *Journal of Pediatric Orthopaedics*, vol. 25, no. 3, pp. 322–325, Jan. 2005, doi: 10.1097/01.BPO.0000152909.16045.38.
[36] F. Firmin and R. Crouch, “Splinting versus casting of ‘torus’ fractures to the distal radius in the paediatric patient presenting at the emergency department (ED): a literature review,” *Int Emerg Nurs*, vol. 17, no. 3, pp. 173–178, Jan. 2009, doi: 10.1016/J.IENJ.2009.03.006.
[37] E. Taylor, J. Hanna, and H. J. C. R. Belcher, “Splinting of the hand and wrist,” *Curr Orthop*, vol. 17, no. 6, pp. 465–474, Dec. 2003, doi: 10.1016/J.CUOR.2003.09.001.
[38] F. Blaya, R. O. D’amato, P. S. Pedro, J. A. Juanes, J. A. Lopez-Silva, and J. G. Lagándara, “Study, design and prototyping of arm splint with additive manufacturing process,” in *ACM International Conference Proceeding Series*, 2017, vol. Part F132203. doi: 10.1145/3144826.3145407.
[39] L. Pugliese *et al.*, “The clinical use of 3D printing in surgery,” *Updates Surg*, vol. 70, no. 3, pp. 381–388, Jan. 2018, doi: 10.1007/S13304-018-0586-5.
[40] R. A. Katkar, R. M. Taft, and G. T. Grant, “3D Volume Rendering and 3D Printing (Additive Manufacturing),” *Dent Clin North Am*, vol. 62, no. 3, pp. 393–402, Jan. 2018, doi: 10.1016/J.CDEN.2018.03.003.
[41] D. A. Schwartz and K. A. Schofield, “Utilization of 3D printed orthoses for musculoskeletal conditions of the upper extremity: A systematic review,” *Journal of Hand Therapy*, vol. 11, p. 43, 2021, doi: 10.1016/j.jht.2021.10.005.

[42] F. Górski, R. Wichniarek, W. Kuczko, M. Zukowska, M. Lulkiewicz, and P. Zawadzki, “Experimental Studies on 3D Printing of Automatically Designed Customized Wrist-Hand Orthoses,” *Materials 2020, Vol. 13, Page 4091*, vol. 13, no. 18, p. 4091, Sep. 2020, doi: 10.3390/MA13184091.
[43] F. Górski *et al.*, “Automated Design of Customized 3D-Printed Wrist Orthoses on the Basis of 3D Scanning,” 2016, pp. 1133–1143. doi: 10.1007/978-3-030-27053-7_97.
[44] A. M. Paterson, R. Bibb, R. I. Campbell, and G. Bingham, “Comparing additive manufacturing technologies for customised wrist splints,” *Rapid Prototyp J*, vol. 21, no. 3, 2015, doi: 10.1108/RPJ-10-2013-0099.
[45] M. Keller, A. Guebeli, F. Thieringer, and P. Honigmann, “In-hospital professional production of patient-specific 3D-printed devices for hand and wrist rehabilitation,” *Hand Surgery and Rehabilitation*, vol. 40, no. 2. 2021. doi: 10.1016/j.hansur.2020.10.016.
[46] M. A. de Souza, C. Schmitz, M. M. Pinhel, J. A. P. Setti, and P. Nohama, “Proposal of custom made wrist orthoses based on 3D modelling and 3D printing,” *Proceedings of the Annual International Conference of the IEEE Engineering in Medicine and Biology Society, EMBS*, pp. 3789–3792, Sep. 2017, doi: 10.1109/EMBC.2017.8037682.
[47] D. S. Chae *et al.*, “The functional effect of 3D-printing individualized orthosis for patients with peripheral nerve injuries: Three case reports,” *Medicine*, vol. 99, no. 16, 2020, doi: 10.1097/MD.0000000000019791.
[48] S. J. Kim, S. J. Kim, Y. H. Cha, K. H. Lee, and J. Y. Kwon, “Effect of personalized wrist orthosis for wrist pain with three-dimensional scanning and printing technique: A preliminary, randomized, controlled, open-label study,” *Prosthet Orthot Int*, vol. 42, no. 6, 2018, doi: 10.1177/0309364618785725.
[49] H. Kim and S. Jeong, “Case study: Hybrid model for the customized wrist orthosis using 3D printing,” *Journal of Mechanical Science and Technology*, vol. 29, no. 12, 2015, doi: 10.1007/s12206-015-1115-9.
[50] T. Galeta, P. Raos, J. Stojšić, and I. Pakši, “Influence of structure on mechanical properties of 3D printed objects,” in *Procedia Engineering*, 2016, vol. 149. doi: 10.1016/j.proeng.2016.06.644.
[51] Md. Q. Tanveer, A. Haleem, and M. Suhaib, “Effect of variable infill density on mechanical behaviour of 3-D printed PLA specimen: an experimental investigation,” *SN Appl Sci*, vol. 1, no. 12, p. 1701, 2019, doi: 10.1007/s42452-019-1744-1.
[52] M. M. Hanon, R. Marczis, and L. Zsidai, “Influence of the 3D printing process settings on tensile strength of PLA and HT-PLA,” *Periodica Polytechnica Mechanical Engineering*, vol. 65, no. 1, 2021, doi: 10.3311/PPme.13683.
[53] S. T. Dwiyati, A. Kholil, R. Riyadi, and S. E. Putra, “Influence of layer thickness and 3D printing direction on tensile properties of ABS material,” in *Journal of Physics: Conference Series*, 2019, vol. 1402, no. 6. doi: 10.1088/1742-6596/1402/6/066014.
[54] G. Ćwikła, C. Grabowik, K. Kalinowski, I. Paprocka, and P. Ociepka, “The influence of printing parameters on selected mechanical properties of FDM/FFF 3D-printed parts,” in *IOP Conference Series: Materials Science and Engineering*, 2017, vol. 227, no. 1. doi: 10.1088/1757-899X/227/1/012033.
[55] T. Letcher and M. Waytashek, “Material property testing of 3D-printed specimen in pla on an entry-level 3D printer,” in *ASME International Mechanical Engineering Congress and Exposition, Proceedings (IMECE)*, 2014, vol. 2A. doi: 10.1115/IMECE2014-39379.
[56] P. Hoogervorst *et al.*, “A Biomechanical Comparison of Fiberglass Casts and 3-Dimensional–Printed, Open-Latticed, Ventilated Casts,” *Hand*, vol. 15, no. 6, 2020, doi: 10.1177/1558944719831341.
[57] F. Buonamici *et al.*, “A practical methodology for computer-aided design of custom 3D printable casts for wrist fractures,” *Visual Computer*, vol. 36, no. 2, 2020, doi: 10.1007/s00371-018-01624-z.
[58] A. Cazon, S. Kelly, A. M. Paterson, R. J. Bibb, and R. I. Campbell, “Analysis and comparison of wrist splint designs using the finite element method: Multi-material three-dimensional printing compared to typical existing practice with thermoplastics,” *Proc Inst Mech Eng H*, vol. 231, no. 9, 2017, doi: 10.1177/0954411917718221.
[59] Y. Zheng *et al.*, “Effects of a 3D-printed orthosis compared to a low-temperature thermoplastic plate orthosis on wrist flexor spasticity in chronic hemiparetic stroke patients: a randomized controlled trial.,” *Clin Rehabil*, vol. 34, no. 2, pp. 194–204, Feb. 2020, doi: 10.1177/0269215519885174.
[60] G. Angelucci and F. Mollaioli, “Voronoi-like grid systems for tall buildings,” *Front Built Environ*, vol. 4, 2018, doi: 10.3389/fbuil.2018.00078.
[61] M. J. Silva and L. J. Gibson, “The effects of non-periodic microstructure and defects on the compressive strength of two-dimensional cellular solids,” *Int J Mech Sci*, vol. 39, no. 5, 1997, doi: 10.1016/s0020-7403(96)00065-3.

[62] M. Kalantari and M. Nechifor, “Accuracy and utility of the Structure Sensor for collecting 3D indoor information,” *Geo-Spatial Information Science*, vol. 19, no. 3, 2016, doi: 10.1080/10095020.2016.1235817.
[63] C. L. Ventola, “Medical Applications for 3D Printing: Current and Projected Uses.,” 2014.
[64] A. S. Boyd, H. J. Benjamin, and C. Asplund, “Principles of casting and splinting,” *American Family Physician*, vol. 79, no. 1. 2009.
[65] M. Gedeon, “Yield Strength and Other Near-Elastic Properties”.
[66] U.S. Department of Health and Human Services Food and Drug Administration Center for Devices and Radiological Health Center for Biologics Evaluation and Research, “Use of International Standard ISO 10993-1, ‘Biological evaluation of medical devices - Part 1: Evaluation and testing within a risk management process,’” *September 4*. 2020.
[67] S. P. Timoshenko, “ X. On the transverse vibrations of bars of uniform cross-section ,” *The London, Edinburgh, and Dublin Philosophical Magazine and Journal of Science*, vol. 43, no. 253, 1922, doi: 10.1080/14786442208633855.
[68] S. Balsky, “Rehabilitation protocol for undisplaced Colles ’ fractures following cast removal,” *J Can Chiropr Assoc.*, vol. 44, no. 416, 2000.
[69] K. Summers and S. M. Fowles, *Colles’ Fracture*. 2022.
[70] E. M. M. van Lieshout *et al.*, “Personalized 3D-printed forearm braces as an alternative for a traditional plaster cast or splint; A systematic review.,” *Injury*, vol. 53 Suppl 3, pp. S47–S52, Nov. 2022, doi: 10.1016/j.injury.2022.07.020.
[71] C. Pool, “Colles’s fracture. A prospective study of treatment.,” *J Bone Joint Surg Br*, vol. 55, no. 3, pp. 540–544, Aug. 1973.
[72] H. D. Stewart, A. R. Innes, and F. D. Burke, “Functional cast-bracing for Colles’ fractures. A comparison between cast-bracing and conventional plaster casts.,” *J Bone Joint Surg Br*, vol. 66, no. 5, pp. 749–53, Nov. 1984, doi: 10.1302/0301-620X.66B5.6389558.
[73] H. H. Handoll and R. Madhok, “Conservative interventions for treating distal radial fractures in adults,” *Cochrane Database of Systematic Reviews*, 2003, doi: 10.1002/14651858.cd000314.
[74] R. H. Plaut, “Determining effective bending stiffness of fabrics and other materials from tests involving an added weight:,” *https://doi.org/10.1177/0040517519858772*, vol. 90, no. 1, pp. 101–109, Jan. 2019, doi: 10.1177/0040517519858772.
[75] S. L. Delp, A. E. Grierson, and T. S. Buchanan, “Maximum isometric moments generated by the wrist muscles in flexion-extension and radial-ulnar deviation.,” *J Biomech*, vol. 29, no. 10, pp. 1371–5, Oct. 1996, doi: 10.1016/0021-9290(96)00029-2.
[76] S. F. Baumbach, R. Schmidt, P. Varga, T. Heinz, V. Vécsei, and P. K. Zysset, “Where is the distal fracture line location of dorsally displaced distal radius fractures?,” *Journal of Orthopaedic Research*, vol. 29, no. 4, 2011, doi: 10.1002/jor.21268.
[77] S. F. Baumbach *et al.*, “Assessment of a novel biomechanical fracture model for distal radius fractures.,” *BMC Musculoskelet Disord*, vol. 13, 2012, doi: 10.1186/1471-2474-13-252.
[78] C. B. Corsino, R. A. Reeves, and R. N. Sieg, *Distal Radius Fractures*. 2022.
[79] K. S. Farbman, R. J. Vinci, W. R. Cranley, W. R. Creevy, and H. Bauchner, “The role of serial radiographs in the management of pediatric torus fractures,” *Arch Pediatr Adolesc Med*, vol. 153, no. 9, 1999, doi: 10.1001/archpedi.153.9.923.
[80] J. J. Sinikumpu and Y. Nietosvaara, “Treatment of Distal Forearm Fractures in Children,” *Scandinavian Journal of Surgery*, vol. 110, no. 2, 2021, doi: 10.1177/1457496920983104.
[81] A. P. Gleeson, M. J. Stuart, B. Wilson, and B. Phillips, “Ultrasound assessment and conservative management of inversion injuries of the ankle in children: plaster of Paris versus Tubigrip.,” *J Bone Joint Surg Br*, vol. 78, no. 3, pp. 484–7, May 1996.
[82] S. Mehta and E. N. Kubiak, “Journal of Orthopaedic Trauma,” *Clin Orthop Relat Res*, vol. 466, no. 10, 2008, doi: 10.1007/s11999-008-0419-9.
[83] N. Gonzalez, J.-M. P. Lucas, A. Winegar, J. den Haese, and P. Danahy, “A Review of Pediatric Distal Radius Buckle Fractures and the Current Understanding of Angled Buckle Fractures.,” *Cureus*, vol. 14, no. 5, p. e24943, May 2022, doi: 10.7759/cureus.24943.
[84] B. D. Waters PM, *Fractures of the distal radius and ulna.*, 7th ed. In Rockwood and Wilkins’ Fractures in Children, 2010.
[85] A. Plint *et al.*, “Wrist buckle fractures: A survey of current practice patterns and attitudes toward immobilization,” *Canadian Journal of Emergency Medicine*, vol. 5, no. 2, 2003, doi: 10.1017/S1481803500008228.

[86] Á. T. Schlégl, R. Told, K. Kardos, A. Szőke, Z. Ujfalusi, and P. Maróti, “Evaluation and Comparison of Traditional Plaster and Fiberglass Casts with 3D-Printed PLA and PLA-CaCO3 Composite Splints for Bone-Fracture Management.,” *Polymers (Basel)*, vol. 14, no. 17, Aug. 2022, doi: 10.3390/polym14173571.
[87] M. I. Mohammed and P. Fay, “Design and additive manufacturing of a patient specific polymer thumb splint concept,” in *Solid Freeform Fabrication 2018: Proceedings of the 29th Annual International Solid Freeform Fabrication Symposium - An Additive Manufacturing Conference, SFF 2018*, 2020.
[88] J. S. Grüschke, H. A. Reinders-Messelink, A. E. van der Vegt, and C. K. van der Sluis, “User perspectives on orthoses for thumb carpometacarpal osteoarthritis,” *Journal of Hand Therapy*, vol. 32, no. 4, 2019, doi: 10.1016/j.jht.2018.04.006.
[89] R. Rizza, X. Liu, and V. Anewenter, “Effect of Window and Hole Pattern Cut-Outs on Design Optimization of 3D Printed Braces.,” *Frontiers in rehabilitation sciences*, vol. 3, p. 889905, 2022, doi: 10.3389/fresc.2022.889905.
[90] R. Xu, Z. Wang, T. Ma, Z. Ren, and H. Jin, “Effect of 3D printing individualized ankle-foot orthosis on plantar biomechanics and pain in patients with plantar fasciitis: A randomized controlled trial,” *Medical Science Monitor*, vol. 25, 2019, doi: 10.12659/MSM.915045.
[91] R. Xu *et al.*, “Comparative study of the effects of customized 3D printed insole and prefabricated insole on plantar pressure and comfort in patients with symptomatic flatfoot,” *Medical Science Monitor*, vol. 25, 2019, doi: 10.12659/MSM.916975.
[92] S. Telfer, J. Woodburn, A. Collier, and P. R. Cavanagh, “Virtually optimized insoles for offloading the diabetic foot: A randomized crossover study,” *J Biomech*, vol. 60, 2017, doi: 10.1016/j.jbiomech.2017.06.028.
[93] Z. Liu, P. Zhang, M. Yan, Y. Xie, and G. Huang, “Additive manufacturing of specific ankle-foot orthoses for persons after stroke: A preliminary study based on gait analysis data,” *Mathematical Biosciences and Engineering*, vol. 16, no. 6, 2019, doi: 10.3934/mbe.2019410.
[94] A. P Fitzpatrick, “Design of a Patient Specific, 3D printed Arm Cast,” *KnE Engineering*, vol. 2, no. 2, 2017, doi: 10.18502/keg.v2i2.607.
[95] Y. Chen *et al.*, “Application of 3D-Printed Orthopedic Cast for the Treatment of Forearm Fractures: Finite Element Analysis and Comparative Clinical Assessment.,” *Biomed Res Int*, vol. 2020, p. 9569530, 2020, doi: 10.1155/2020/9569530.

Appendix 1

RESEARCH PROTOCOL

Protocol titel: Pilot: haalbaarheid van implementatie van 3D geprinte polsspalken voor de behandeling van kinderen met greenstick- en torusfracturen

Korte titel: Pilot 3D prints bij greenstickfracturen
Versie: 2
Datum: 16-02-2022

Hoofdonderzoeker (gepromoveerd)/uitvoerder)
Dr. J.M.M. Heyligers, Vaatchirurg
j.heyligers@etz.nl
+31(0)13 221 6087
M. Bemelman, Traumachirurg
m.bemelman@etz.nl
+31(0)13 221 6587

Uitvoerend onderzoeker
Koen Storck, Student Technical Medicine
k.c.g.storck@student.utwente.nl
+31(0)6 1788 7639

Datum en handtekening
16/02/2022

Samenvatting

Motivering

Een fractuur van de radius is de meest voorkomende fractuur in Nederland. De gouden standaard voor de behandeling van polsfracturen is circulair onderarm gips. Nadelen van de behandeling met gips zijn het ontstaan zweten en het ontbreken van ventilatie, waardoor jeuk, stank en huidproblemen kunnen ontstaan. 3D geprinte polsspalken zouden een goede oplossing kunnen zijn voor deze nadelen. Verschillende commerciële instanties bieden deze service reeds aan in Nederland. Het afgelopen jaar is binnen het ETZ ruim onderzoek gedaan naar het in huis produceren van dit soort polsspalken. Klinische implementatie is hierbij de volgende stap. Het meest uitdagende is de logistieke afhandeling hiervan. Na presentatie dient de spalk zo snel mogelijk beschikbaar te worden voor de patiënt. Greenstick- en torusfracturen worden traditioneel behandeld met gips of een drukverband. Hoewel voor functieherstel is aangetoond dat eigenlijk geen behandeling nodig is, wordt immobilisatie toegepast ter pijnstilling. Vanwege het stabiele karakter van greenstick- en torusfracturen en minimale zwelling bij kinderen is deze groep uitermate geschikt voor de implementatie van de 3D geprinte polsspalken ter behandeling van deze polsfracturen. De voordelen van een geprinte spalk, minder zweten en jeuk en het nat mogen worden is ook voor deze groep erg belangrijk.

Doelstellingen

- Is het implementeren van 3D geprinte polsspalken binnen de workflow van het ETZ logistiek haalbaar en wat is de (extra) tijdsbelasting voor kliniek en patiënt?
- Komen de theoretische voordelen van 3D geprinte polsspalken (lichtgewicht, waterbestendig, ventilatie, hygiëne, gepersonaliseerd) tot uiting binnen de praktische toepassing?
- Hoe bevalt de inzet van 3D geprinte polsspalken in het dagelijks gebruik bij kinderen en ouders?

Studie design:

Single center prospectieve pilotstudie.

Studie populatie:

Kinderen van 4 tot en met 15 jaar met een greenstick- of torusfractuur die zich melden op de SEH. Omdat het een PILOT studie betreft, bestaat de populatie uit minimaal 5 patiënten.

Interventie:

Behandeling met 3D geprinte polsspalk in plaats van onderarm gips of drukverband.

Methode:

Na melding op de SEH worden patiënt en ouders gevraagd vrijwillig mee te doen aan de studie. In het geval van inclusie, wordt op de SEH een 3D scan van de onderarm met de fractuur gemaakt. Patiënten krijgen vervolgens een tijdelijk kalkgips. Binnen 12 uur wordt een 3D geprinte spalk geprint. Binnen 24 uur melden patiënten zich weer in het ziekenhuis om het kalkgips te verwijderen en de spalk aan te meten. Patiënten en ouders krijgen instructies mee naar huis. Na twee weken worden patiënten en ouders teruggezien voor een evaluatiegesprek. Hierbij wordt een functiemeting uitgevoerd en wordt bij zowel de kinderen als de ouders een vragenlijst afgenomen.

Primaire studie parameters/ eindpunten:

Primair wordt er gekeken naar de inpassing van de 3D geprinte polsspalken binnen de huidige workflow van het ETZ. Hierbij wordt met name gekeken naar de tijdsbelasting rondom het design en de productie en naar het aantal contactmommentenen. Verder wordt de ervaring van de patiënten en ouders over de behandeling met 3D geprinte polsspalken gemeten door middel van vragenlijsten.

Aard en omvang van de belasting, risico's en voordelen voor deelnemers geassocieerd met deelname (zowel individueel als voor de groep):

Extra belasting voor de deelnemers is er niet. Er zijn geen extra follow-up momenten naast de reguliere gips behandeling. Ook bij de laatst genoemde behandeling wordt de patiënt tussentijds terug gezien om het gips te controleren. Verwachte voordelen liggen op het gebied van hygiëne, ventilatie, gewicht en gebruiksgemak. Er bestaat een minimaal risico op huidirritatie, drukplekken, vensteroedeem of huidschade door breken van de spalk bij ongevallen. Dit risico is niet anders dan bij gips.

Introductie en motivering

Polsfracturen zijn de meest voorkomende fracturen bij kinderen. De distale radius is betrokken bij 30-35% van alle geregistreerde fracturen bij kinderen tussen 0 en 15 jaar, waarbij de meerderheid van de fracturen bestaat uit greenstick- en torusfracturen. [1, 2, 3]. De hogere compliantie van pediatrisch bot zorgt ervoor dat botten de neiging hebben om eerder te buigen dan te breken. Hierdoor zijn fracturen bij kinderen vaker incomplete fracturen, zoals greenstick- en torusfracturen [4]. Deze fracturen zijn over het algemeen stabiel en niet snel geneigd te verplaatsen [5].

De gouden standaard voor de behandeling van distale radiusfracturen is circulair onderarm gips voor 2 tot 3 weken, afhankelijk van het type fractuur [6]. Eerder onderzoek heeft echter aangetoond dat voor de behandeling van greenstick- en torusfracturen drukverband ter pijnstilling ook voldoende is voor herstel en dat immobilisatie eigenlijk niet noodzakelijk is [7, 8]. Op dit moment wordt de behandeling van greenstick-en torusfracturen binnen het ETZ dan ook gebaseerd op de voorkeur van de patiënt en de ouders. In de praktijk betekent dit meestal kortdurend gips.

Zowel de behandeling met gips als met drukverband kennen echter een aantal nadelen, met name op het gebied van hygiëne, ventilatie en inspectie van de huid. Beide mogen niet nat worden, dus douchen en zwemmen zijn geen optie zonder de nodige aanpassingen [9]. Verder zorgen beide vaak voor jeuk en zweten, waardoor stank en mogelijk huidproblemen kunnen ontstaan. De slechte hygiëne en het gewicht bij gips zijn de twee zaken die patiënten het meest tegenstaan aan de traditionele behandeling [9, 10, 11].

Drie dimensionaal (3D) geprinte polsspalken zouden een oplossing kunnen zijn voor deze problemen, terwijl wel de immobiliserende en pijnstillende werking bereikt kan worden. Met behulp van 3D printen kan een opengewerkte, lichtgewicht, waterbestendige en persoonlijke spalk gemaakt worden.

Landelijk worden 3D geprinte spalken ruim aangeboden door commerciële bedrijven, bijvoorbeeld gekoppeld aan de St. Maartenskliniek in Nijmegen. Binnen het ETZ is hiervoor meer dan een jaar onderzoek gedaan naar materiaaleigenschappen, designmogelijkheden, mechanische eigenschappen en comfort. De volgende stap is om de haalbaarheid van klinische implementatie (logistiek) te onderzoeken. Greenstick- en torusfracturen zijn vanwege het stabiele karakter geschikt voor deze klinische vervolgstap. Aangezien de spalk op basis van een 3D scan van de onderarm gemaakt wordt, kan zwelling ervoor zorgen dat de spalk bij afname van de zwelling minder goed aansluit op de arm. Bij kinderen met deze typen fracturen is er echter weinig sprake van zwelling, wat dit ook een geschikte groep maakt voor de eerste klinische vervolgstap.

Tijdens voorgaand fantoomonderzoek binnen het ETZ is aangetoond dat de verplaatsing van de arm in de spalk niet significant verschilt ten opzichte van de verplaatsing in gips op basis van de krachten die met een gezonde, volwassen, mannelijke pols gegenereerd kunnen worden [12]. Hiermee is aangetoond dat het stabilisatievermogen van de spalk vergelijkbaar is met dat van gips. Bij deze testen zijn bewust realistische klinische waarden overschreden, zodat een veiligheidsmarge van de te weerstane krachten gegarandeerd kan worden zonder dat er vervorming van de spalk optreedt.

Doelstellingen

Het doel van deze studie is om de haalbaarheid van klinische implementatie van 3D geprinte polsspalken te onderzoeken, alsmede de tevredenheid over de praktische toepassing van deze spalken te onderzoeken.

Doelstellingen:

- Is het implementeren van 3D geprinte polsspalken binnen de workflow van het ETZ logistiek haalbaar en wat is de (extra) tijdsbelasting voor kliniek en patiënt?
- Komen de theoretische voordelen van 3D geprinte polsspalken (lichtgewicht, waterbestendig, ventilatie, hygiëne, gepersonaliseerd) tot uiting binnen de praktische toepassing?
- Hoe bevalt de inzet van 3D geprinte polsspalken in het dagelijks gebruik bij kinderen en ouders?

Studie design

Dit is een prospectieve pilot in één level 1 traumacentrum, waarin de haalbaarheid van de inzet van 3D geprinte polsspalken bij de behandeling van kinderen met een greenstick- of torusfractuur onderzocht wordt. De patiënten krijgen de keus voor een spalk als interventie in plaats van de traditionele behandeling met drukverband of gips. Zowel de ouders als de kinderen krijgen een vragenlijst om de ervaring te beoordelen.

Studie populatie

De studiepopulatie zal bestaan uit een vijftal patiënten die op de spoedeisende hulp (SEH) van het ETZ, locatie St. Elisabeth, gediagnostiseerd zijn met een greenstick- of torusfractuur.

Inclusiecriteria:

- Patiënten die zich melden op de SEH met een greenstick- of torusfractuur.
- Kinderen tussen 4-15 jaar.

Exclusiecriteria:

- Ouders en/of kind hebben niet voldoende kennis van de Nederlandse taal.
- Kind kan niet voldoende communiceren (pijn/discomfort aangeven).
- Kind is bekend met een huid aandoening: bijvoorbeeld eczeem, psoriasis.

Inclusiemethode

De assistenten en verpleegkundigen van de SEH signaleren als eerste de binnenkomst van een patiënt met een greenstick- of torusfractuur. Inclusie zal via deze weg verlopen. De assistent of verpleegkundige belt de uitvoerend onderzoeker zodra een patiënt binnenkomt die voor inclusie in aanmerking komt.
De uitvoerend onderzoeker zal vervolgens op de SEH uitleg verzorgen aan de ouders en het kind over de inhoud en gang van zaken van de studie en vragen om informed consent (en mogelijk assent). Hierbij zullen de belangrijkste rechten en plichten worden besproken zodat men een gegronde overweging kan maken met betrekking tot deelname. Figuur 1 toont een stroomdiagram met de inclusiestappen.

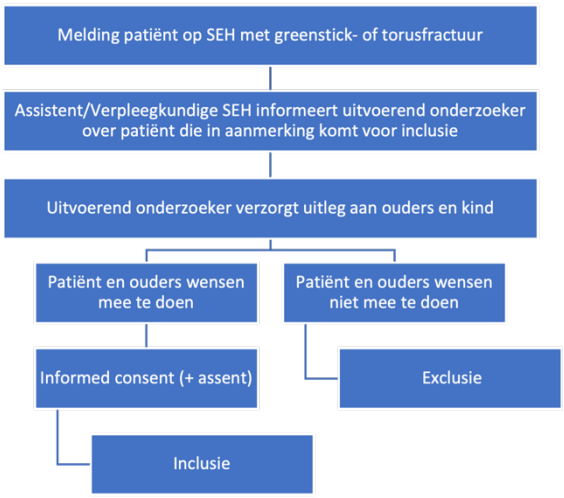

Figuur 1: Inclusiestappen

Methode

Studieprocedure

Zodra een patiënt geïncludeerd is, zal er een 3D scan gemaakt worden van de onderarm. Dit gebeurt met een 3D scanner op basis van LED en infrarood licht (Einscan H [SHINING 3D® Tech. Co., Ltd., Hangzhou, China]). Het maken van de scan neemt ongeveer 1 minuut in beslag en is volstrekt pijnloos, zonder enige vorm van straling. Op de SEH krijgt de patiënt vervolgens een tijdelijk kalkgips, zoals dat gebruikelijk is in het weekend en avonduren. Vervolgens mag de patiënt naar huis om binnen 48 uur terug komen op de poli voor het aanmeten van de spalk.

In de 24-48 uur tussen binnenkomst op de SEH en terugkomst op de poli, wordt op basis van de 3D scan van de onderarm een spalk ontworpen en geprint. Het design van de spalk gebeurt in Rhino 6 [Rhinoceros, Seattle, USA] en Meshmixer® [AutoDesk, Inc., San Rafael, USA]. Dit proces neemt 1-2 uur in beslag, waarna in zo'n 12-18 uur een spalk geprint kan worden (de precieze tijd is afhankelijk van de omtrek van de arm en lengte van de spalk). De spalk wordt geprint met een stereolithografie (SLA) printer (FormLabs 2 of FormLabs 3 [FormLabs Inc., Somerville, USA]) met standard kleurenhars (Color resin V1, FormLabs [FormLabs Inc., Somerville, USA]). De nabewerking (verwijderen van supportmateriaal, inspectie en uitharden) kost 90 minuten. Binnen 24-48 uur is een spalk klaar voor aanmeting. De precieze ontwerp- en productietijd wordt per spalk bijgehouden. De spalk bestaat uit twee delen, die bij elkaar gehouden worden door twee klittenbanden door speciaal ontworpen en geprinte sleuven in de spalken. De spalk kan geprint worden in vier kleuren: roze, blauw, groen en oranje. De kleurkeuze wordt bij opname op de SEH voorgelegd aan de patiënt.

Binnen 48 uur wordt de patiënt teruggezien op de poli, waar het kalkgips wordt verwijderd en de spalk aangemeten wordt. De eerste dagen wordt de arm met behulp van een mitella hooggehouden. De patiënt en ouders krijgen verdere instructies uitgelegd en per folder mee naar huis. Het belangrijkst is hierbij dat beweging mag op geleide van de pijn. Verder mag er gedoucht en gezwommen worden met de spalk. De ouders wordt gevraagd dagelijks een korte inspectie uit te voeren van de huid. Hierbij dienen de ouders op te letten of er irritatie, drukpunten of oedeem te zien zijn. Indien het geval dan noteren zij dat (het moment, beschrijving van de visuele inspectie) en maken hier, indien mogelijk, een foto van. De ouders mogen en kunnen altijd de spalk verwijderen door het losmaken van het klittenband. Als de ouders de spalk los hebben gemaakt dient er contact opgenomen te worden met de supervisor van het onderzoek (daarnaast wordt dit vastgelegd in EPIC). Hiervoor wordt het telefoonnummer van de supervisor (Mike Bemelman) meegegeven. Ten slotte de patiënten (en ouders van de patiënten) mogen altijd bellen met vragen en klachten of terug mogen komen voor een wissel naar gips of drukverband. Indien de wens is om te wisselen van behandeling zal dit worden verwerkt in Epic.

Na twee weken worden de patiënten met ouders teruggezien op de poli voor evaluatie. Hierbij wordt een functiemeting van de aangedane pols uitgevoerd (de uitkomsten van de functietesten worden vastgelegd in EPIC). De functie test bestaat uit:

- Dorsaalflexie: handen zover mogelijk naar boven
- Plantairflexie: handen zover mogelijk naar beneden
- Ulnair deviatie: handen zover mogelijk naar pinkzijde
- Radiaal deviatië: handen zover mogelijk naar duimzijde
- Pro/supinatie: linksom en rechtsom

Daarnaast wordt zowel de kinderen als de ouders gevraagd een vragenlijst in te vullen. Hierbij wordt voor de kinderen met behulp van een VAS-score (schaal van 1-5, aan de hand van smileys) uitgevraagd hoe zij de verschillende dagelijkse handeling en pijn hebben ervaren met de spalk. Aan de ouders wordt de ervaring uitgevraagd aan de hand een VAS-score (schaal 1-10, getallen) en worden mogelijke aanpassingen en voorkeur voor toekomstige behandeling uitgevraagd.

Studieparameters

De studieparameters zullen worden bewaard in een geanonimiseerd Excel bestand (d.m.v. een sleutelbestand).

Primaire parameters

Primair wordt er gekeken naar de inpassing van de 3D geprinte polsspalken binnen de huidige workflow van het ETZ en de ervaring van de patiënten en ouders over de behandeling met 3D geprinte polsspalken.

1. Tijdsbelasting ontwerp en productie van de polsspalk en aantal contactmomenten
2. Scores ervaring patiënt
3. Scores ervaring ouders

Secundaire parameters

1) Patiëntparameters: leeftijd, geslacht, lateraliteit fractuur, dominante arm, type fractuur (greenstick of torus), aanwezigheid van complicaties (irritatie, oedeem, huidschade, en spalk intact na laatste contact moment).
2) Spalkparameters: Design-, print-, nabewerkingstijd (in uren), materiaalkosten (€)

Data analyse plan

Gegevens van patiënten worden op papier verzameld in afgesloten kast in afgesloten ruimte, analyse zal naar gelang het aantal patiënten plaatsvinden via Researchmanager of Excel. En verdere analyse zal worden gedaan met SPSS (Statistical Package for Social Sciences, versie 25 [IBM Corp., Chicago IL, USA]) worden de gegevens geanonimiseerd (waar dat voor zover nog niet gedaan was).

De resultaten per patiënt worden binnen het ETZ opgeslagen in Excel. Hierin worden patiëntgegevens, de uitkomsten van de vragenlijsten en tijdsbelasting ingevuld. Er zal een sleutelbestand gemaakt worden met daarin het patiëntnummer en de geboortedatum die gekoppeld zijn aan een coderingsnummer. In het andere bestand worden de coderingsnummers gekoppeld aan de (primaire en secundaire) parameters. Dit zal worden bewaard op de laptop van de trauma afdeling die alleen te gebruiken is door de hoofdonderzoeker.

Per deelvraag uit de vragenlijst wordt de gemiddelde score en spreiding berekend voor analyse van de doelstellingen. Aangezien er geen controlegroep is, worden de scores door middel van beschrijvende statistiek (histogram of boxplot of soortgelijke statistiek) geanalyseerd.

Aard en omvang van de belasting, risico's en voordelen voor deelnemers geassocieerd met deelname (zowel individueel als voor de groep):

Aangezien aangetoond is dat het stabiliseringsvermogen van de spalk vergelijkbaar is met gips, wordt geen risico verwacht met betrekking tot herstel. Ook omdat al aangetoond is in eerder onderzoek dat immobilisatie voor functieherstel niet noodzakelijk is [7, 8]. De te verwachten voordelen liggen op het gebied van hygiëne, ventilatie, gewicht en gebruiksgemak. Er wordt verwacht dat de stank en jeuk minimaal zullen zijn en dat een groot voordeel is dat er met de spalk zonder aanpassingen gedoucht en gezwommen kan worden. Bijkomend voordeel is dat de polsspalk lichtgewicht en personaliseerbaar is.

Er bestaat een minimaal risico op het ontstaan van huidirritatie, drukplekken of vensteroedeem. Hoewel bij eerder comfort onderzoek geen problemen geconstateerd werden op dit gebied, kan dit niet met zekerheid uitgesloten worden. Verder zou bij hoge impact de spalk kunnen breken. Dit breekpunt zal door middel van klinisch gebruik niet bereikt worden, maar bij ongelukken en ongevallen kan niet uitgesloten worden dat de spalk breekt. Hierbij kan versplintering ontstaan wat schade zou kunnen toebrengen aan de huid, zoals kleine prikverwondingen. Dit risico is vergelijkbaar met gips.

De tijdsbelasting van de patiënt en ouders is analoog aan conventionele gipsbehandeling. Feitelijk is er geen extra tijdsbelasting. Bij de traditionele behandeling krijgt de patiënt een tijdelijk kalkgips, waarna de eerstvolgende werkdag het kalkgips gewisseld wordt voor een drukverband of circulair onderarm gips. Bij deze studie komen de patiënten binnen twee dagen na melding op de SEH terug voor de wissel van kalkgips naar 3D geprinte spalk. Bij de traditionele behandeling komen de patiënten na 2 -3 weken terug voor het verwijderen van het gips. Bij de studiegroep zien we de patiënten ook terug voor het verwijderen van de geprinte spalk en het afsluitende gesprek.

Referenties

[1] Brink PRG, Bransz N, Deijkers RLM, van Eerten PV, Kolkman S, van Loon J, Poolman, RW, Segers MJM. Distale radius fracturen – Bijlage: Algemene inleiding. Richtlijnendatabase Federatie Medisch Specialisten. 2010; 1-73.
[2] Sinikumpu JJ, Nietosvaara Y. Treatment of Distal Forearm Fractures in Children. Scand J Surg. 2020; 1-5.
[3] Atanelov Z, Bentley TP. Greenstick Fractures. StatPearls (StatPearls Publishing). 2020.
[4] Corsino CB, Reeves RA, Sieg RN. Distal Radius Fractures. StatPearls (StatPearls Publishing). 2020.
[5] Oakley EA, Ooi KS, Barnett PL. A randomized controlled trial of 2 methods of immobilizing torus fractures of the distal forearm. Pediatr Emerg Care. 2008; 24 (2): 65-70.
[6] Plint AC, Perry JJ, Correll R, Gaboury I, Lawton L. A randomized, controlled trial of removable splinting versus casting for wrist buckle fractures in children. Pediatrics. 2006; 117 (3): 691-697.
[7] Kropman RH, Bemelman M, Segers MJ, Hammacher ER. Treatment of impacted greenstick forearm fractures in children using bandage or cast therapy: a prospective randomized trial. J Trauma. 2010; 68 (2): 425-428.
[8] Plint A, Clifford T, Perry J, Bulloch B, Pusic M, Lalani A, Ali S, Nguyen BH, Joubert G, Millar K. Wrist buckle fractures: a survey of current practice patterns and attitudes toward immobilization. CJEM. 2003; 5 (2): 95-100.
[9] Blaya F, Pedro PS, Silva JL, D'Amato R, Heras ES, Juanes JA. Design of an Orthopedic Product by Using Additive Manufacturing Technology: The Arm Splint. J Med Syst. 2018; 42 (3): 54.
[10] Boutis K, Willan A, Babyn P, Goeree R, Howard A. Cast versus splint in children with minimally angulated fractures of the distal radius: a randomized controlled trial. CMAJ. 2010; 182 (14): 1507-1512.
[11] Graham J, Wang M, Frizzell K, Watkins C, Beredjiklian P, Rivlin M. Conventional vs 3-Dimensional Printed Cast Wear Comfort. Hand (N Y). 2020; 15 (3): 388-392.
[12] Mooij CDY. Mechanical comparison of stabilization capacity between 3D printed wrist casts and traditional plaster casts. ONGEPUBLICEERD. 2021.

Appendix 2

Patiënten informatie 3D geprinte pols spalken bij greenstick- en torusfracturen

Botbreuk

Er is een breuk (greenstickfractuur) of knikje (torusfractuur) in het spaakbeen bij jouw pols vastgesteld.

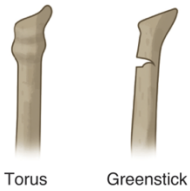

Genezing

Omdat jij jong bent groeien jouw botten snel en geneest een greenstick- of torusfractuur over het algemeen snel (ongeveer 2 weken). In geval van een kleine knikstand, herstelt dit vanzelf, binnen enkele weken tot maanden.

Behandeling

Normaal gesproken wordt een greenstick- of torusfractuur behandeld met een drukverband of gips, naar voorkeur van de patiënt (jij) en de ouders. We willen je vragen of je wilt meedoen aan een onderzoek waarbij jij een, speciaal voor jou gemaakte, 3D geprinte polsspalk krijgt voor de behandeling van je breuk.

Patiëntinstructies

1. Jij krijgt een polsspalk en voor de eerste dagen een draagdoek (mitella), om de pols rust te geven. Rust is belangrijk voor goede genezing en vermindert de pijn. Bij het slapen mag de mitella af. Zodra de pijn het toelaat, hoeft de mitella ook overdag niet meer gedragen te worden.
2. Na een week, zodra de pijn het toelaat, mag jij weer wat meer gaan bewegen, dit voorkomt stijfheid van de arm en verbetert de genezing.
3. De polsspalk zit vast met klittenband. Indien je twijfelt of de spalk goed zit vraag dan aan je ouders om even mee te kijken. Indien nodig mag de spalk afgedaan worden door het losmaken van de klittenband (laat dit door je ouders doen). Wanneer dit gebeurt geven jij of je ouders dit door aan de arts onderaan deze informatiebrief.
4. Douchen en zwemmen kan met de polsspalk. Na het nat worden, mag de spalk kort afgedaan worden om de arm en spalk te drogen. Een andere optie is om met een koude föhn, de arm droog te föhnen.
5. We raden aan iedere dag de huid kort te inspecteren. Doe dit samen met je ouders en let hierbij op zwelling, verkleuring, drukplekken, blaren en wondjes. De spalk mag voor inspectie kort afgedaan worden.
6. Na twee weken zien we jou terug voor controle en mag de spalk af.

Vragen?

Het is belangrijk om te weten dat bij klachten of vragen op ieder moment contact opgenomen mag worden met de supervisor (Mike Bemelman, traumachirurg). Op verzoek van jou en je ouders kan op ieder moment deelname aan het onderzoek beëindigd worden. In overleg met de supervisor wordt de behandeling dan volgens de conventionele richtlijnen voortgezet. Het kan gebeuren dat de supervisor door activiteiten met patiënten niet bereikbaar is, gebruik dan het algemene nummer van het ziekenhuis.

Contact

Mike Bemelman, (traumachirurg, Supervisor onderzoek)
+31(0) 6 296 261 82
+31(0)13 221 65 87 (ziekenhuis)

Appendix 3
Patiënten informatie 3D geprinte pols spalken bij greenstick- en torusfracturen

Botbreuk
Uw kind heeft een twijgbreukje (greenstickfractuur) of knikje (torusfractuur) in het spaakbeen of de ellepijp ter hoogte van de pols opgelopen. Dit is een breukje in het bot, waarbij het botvlies dat om het bot heen ligt, intact is gebleven. Het bot is meer geknikt dan gebroken, waardoor verplaatsing of losraking van de botdelen onwaarschijnlijk is.

Genezing
Omdat kinderen in de groei snel nieuw bot aanmaken, geneest een greenstick- of torusfractuur over het algemeen snel, in ongeveer 2 weken. In geval van een kleine knikstand, herstelt dit vanzelf, binnen enkele weken tot maanden.

Behandeling
Normaal gesproken wordt een greenstick- of torusfractuur behandeld met een drukverband of gips, naar voorkeur van de patiënt en ouders. U en uw kind wordt gevraagd mee te doen aan een onderzoek waarbij een gepersonaliseerde, 3D geprinte polsspalk wordt ingezet voor de behandeling van deze fracturen. Hieronder volgen instructies voor de behandeling.

Patiëntinstructies
7. Uw kind krijgt een polsspalk en voor de eerste dagen een draagdoek (mitella), om de pols rust te geven. Rust is belangrijk voor goede genezing en vermindert de pijn. Bij het slapen mag de mitella af. Zodra de pijn het toelaat, hoeft de mitella ook overdag niet meer gedragen te worden.
8. Na een week, zodra de pijn het toelaat, mag uw kind weer bewegen, dit voorkomt stijfheid van de elleboog en bevordert de genezing.
9. De spalk zit eenvoudig vast met 2 klittenband riempjes. Indien u twijfelt of de spalk goed zit mag u de spalk verwijderen door het losmaken van de klittenband. Neem op dat moment ook direct contact op met de arts onderaan deze informatiebrief. U mag ten alle tijden zowel het mobiele nummer als het ziekenhuis bellen.
10. Douchen en zwemmen kan met de polsspalk. Na het nat worden, mag de spalk kort afgedaan worden om de arm en spalk te drogen. Een andere optie is om met een koude föhn, de arm droog te föhnen.
11. We raden aan iedere dag de huid kort te inspecteren. Let hierbij op zwelling, verkleuring, drukplekken, blaren en wondjes. De spalk mag voor inspectie kort afgedaan worden.
12. Na twee weken zien we uw kind terug voor controle en mag de spalk af.

Vragen?
Het is belangrijk om te weten dat bij klachten of vragen op ieder moment contact opgenomen mag worden met de supervisor (Mike Bemelman, traumachirurg). Op verzoek van patiënt en ouders kan op ieder moment deelname aan het onderzoek beëindigd worden. In overleg met de supervisor wordt de behandeling dan volgens de conventionele richtlijnen voortgezet. Het kan gebeuren dat de supervisor door activiteiten met patiënten niet bereikbaar is, gebruik dan het algemene nummer van het ziekenhuis.

Contact
Mike Bemelman, (traumachirurg, Supervisor onderzoek)
+31(0) 6 296 261 82
+31(0)13 221 65 87 (ziekenhuis)

Appendix 4

Vragenlijst 3D geprinte polsspalk - kind

Versie 1 (20-04-2022) - Type fractuur: ☐ Greenstick ☐ Torus

Over mij:

Ik ben: …… jaar

Ik ben: ☐ een jongen ☐ een meisje

De kant waar mijn pols is gebroken: ☐ links ☐ rechts

Mijn dominante hand is: ☐ links ☐ rechts

---

1. **Had je last van jeuk in de spalk?**

Nooit Bijna nooit Soms Regelmatig Vaak

2. **Had je last van zweten in de spalk?**

Nooit Bijna nooit Soms Regelmatig Vaak

3. **Had je last van stank door de spalk?**

Nooit Bijna nooit Soms Regelmatig Vaak

4. Had je last van pijn door de spalk?

Nooit Bijna nooit Soms Regelmatig Vaak

5. Had je last van huidirritatie door de spalk?

Nooit Bijna nooit Soms Regelmatig Vaak

6. Had je last van het gewicht van de spalk?

Nooit Bijna nooit Soms Regelmatig Vaak

7. Hoe ging het met douchen?

Heel goed Goed Oké Niet goed Slecht

8. Hoe mooi vond je de spalk?

Heel mooi | Mooi | Oké | Niet zo mooi | Lelijk

9. Had je last van de spalk in het dagelijks gebruik?

Nooit | Bijna nooit | Soms | Regelmatig | Vaak

10. Stel je breekt nog een keer je pols, zou je dan opnieuw kiezen voor een deze polsspalk of liever voor gips?

☐ Polsspalk ☐ Gips

11. Wat zou er nog beter kunnen aan de spalk?

.....

.....

Bedankt voor het meedoen aan dit onderzoek!

Appendix 5

Vragenlijst 3D geprinte polsspalk - ouder

Versie 1 (20-04-2022) - Type fractuur: ☐ Greenstick ☐ Torus

Hieronder begint de vragenlijst. Onder de meeste vragen staat een balk met een schaal van 0 tot 10. Op deze balk kunt u aangeven in hoeverre u het eens bent met de vraag (de beschrijving staat onder de scorebalk) door een cijfer te omcirkelen. Bij de overige vragen, kunt u een keuze maken tussen verschillende opties, door het vakje voor het gewenste antwoord aan te kruisen of uw antwoord op de stippellijn in te vullen.

1. In hoeverre werd uw kind beperkt in dagelijkse handelingen door de 3D geprinte polsspalk?

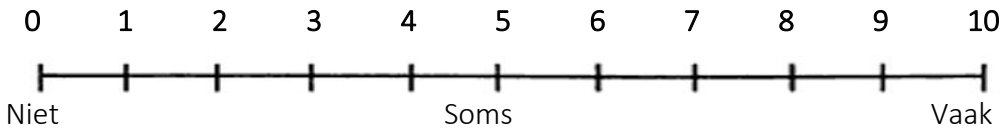

2. Zorgde de 3D geprinte polsspalk voor huidirritatie bij uw kind?

3. Heeft uw kind geklaagd over jeuk?

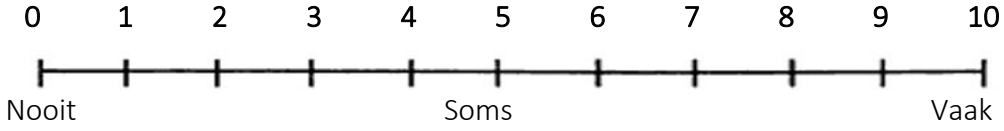

4. Heeft uw kind geklaagd over het gewicht van de 3D geprinte polsspalk?

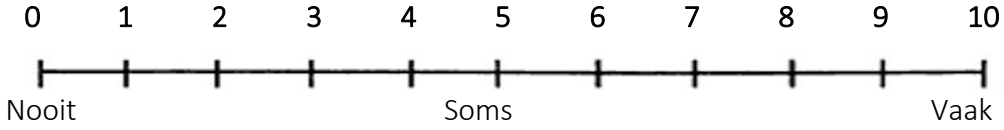

5. Zorgde het dragen van de spalk voor onaangename geuren?

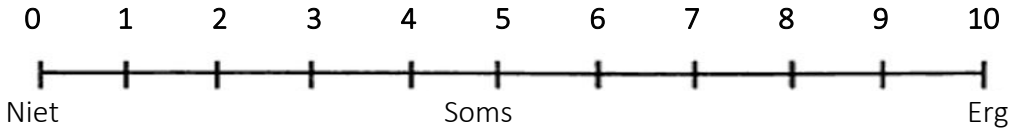

6. Heeft uw kind geklaagd over pijn, veroorzaakt door de 3D geprinte polsspalk?

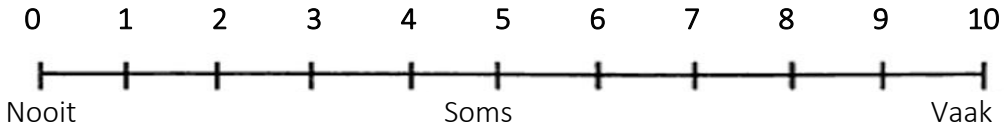

7. Had uw kind last van maceratie (week worden) van de huid na het douchen (of zwemmen) door het dragen van de 3D geprinte polsspalk?

8. Had uw kind last van de 3D geprinte polsspalk met slapen?

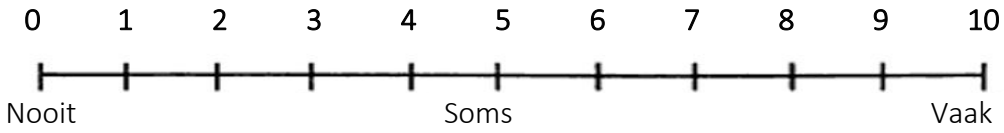

9. Welk cijfer geeft u de behandeling van uw kind met de 3D geprinte polsspalk?

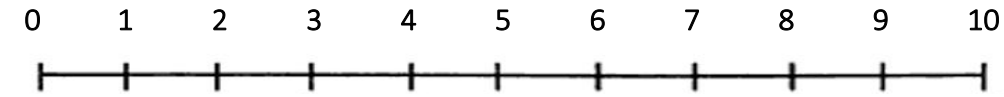

10. Welk cijfer geeft u het uiterlijk van de 3D geprinte polsspalk?

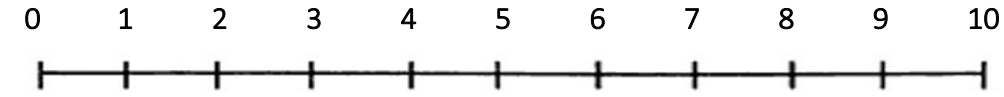

11. Zijn er tijdens de visuele inspectie zaken opgevallen? Zo ja wat? (irritatie, oedeem, huidschade, en spalk intact, en andere opvallende aspecten)

.....

.....

12. Heeft uw kind de spalk tussendoor afgedaan? Zo ja, was dit veroorzaakt door spalk en wat was de oorzaak?

13. Wat vindt u voordelen van de 3D geprinte polsspalk?

14. Wat vindt u nadelen van de 3D geprinte polsspalk?

15. Wat kan er nog verbeterd worden aan de 3D geprinte polsspalk?

16. Zou u in het geval van een volgende breuk bij uw kind voorkeur hebben voor behandeling met een 3D geprinte polsspalk of traditioneel gips?

□ 3D geprinte polsspalk □ Gips

17. Heeft u verder nog op- of aanmerkingen?

Bedankt voor het invullen van de vragenlijst!